8-2017

Instrumental Aspects of Oxygen Sensing: Quantitation and Recalibration of a Biofouled Oxygen Sensor

Marlena Patrick
University of Arkansas, Fayetteville

Instrumental Aspects of Oxygen Sensing: Quantitation and Recalibration of a Biofouled Oxygen Sensor

A dissertation submitted in partial fulfillment
of the requirements for the degree of
Doctor of Philosophy in Chemistry

by

Marlena Patrick
University of Louisiana at Monroe
Bachelor of Science in Chemistry, 2012

August 2017
University of Arkansas

This dissertation is approved for recommendation to the Graduate Council.

Dr. David Paul
Dissertation Director

Dr. Ingrid Fritsch
Committee Member

Dr. Julie Stenken
Committee Member

Dr. Wesley Stites
Committee Member

Abstract

In vivo oxygen sensing is a critical area of research for medical applications, such as ischemic stroke, but this important topic is not fully understood or resolved. In addition, the best method for calibration of in vivo sensors is as yet undetermined. For all implantable devices, biofouling, the adsorption of biological material to the device surface, is another significant problem with no clear or well-defined solution. One method employed is to apply a protective polymer membrane to the sensor surface in order to minimize the adsorption of biological material. The work described here investigates two polymers applied to a gold electrode for oxygen sensing: polyeugenol (PE) and poly-o-phenylenediamine (PoPD). Polyeugenol, while permeable to oxygen, and unhampering to the overall oxygen sensitivity for the sensor, shows polymer instability, and is therefore not applicable to long-term in vivo sensors. PoPD is shown in these works to be both permeable to oxygen and mechanically stable. PoPD was investigated first on 2 mm gold macroelectrodes to increase the fundamental understanding of PoPD for use with oxygen sensors, as well as better understand the biofouling phenomenon when PoPD-coated electrodes were incubated in protein solutions. In addition, PoPD-coated 2 mm gold electrodes were used in an in vivo simulation study in order to illustrate the problem with present calibration methods for in vivo sensors. PoPD was further investigated using gold microelectrodes in biofouling solutions, as microelectrodes are more suitable towards in vivo work; in addition, a method of in situ recalibration of the biofouled PoPD-coated microelectrode was investigated. Fundamental studies described in this dissertation aim to increase the understanding of the biofouling phenomenon through in vitro simulation studies, as well as propose a method to account for and correct the consequences of this phenomenon.

Acknowledgments

I would like to give my sincere gratitude to my advisor Dr. David Paul, for his years of encouragement and guidance throughout this journey. I would not have made it this far without his support, and I am forever grateful for his mentorship. I would also like to thank my parents, Auther and Sheila Robert, for believing in me and always being there for me when I need it most; and my brother Austin Robert, for being the best brother I could have asked for.

I would like to express my appreciation to my committee members, Dr. Julie Stenken, Dr. Ingrid Fritsch, and Dr. Wesley Stites, for their constructive suggestions and discussions, as well as their patience and support along the way. I am grateful for support from the Paul group for their collaborative discussions and for helping ease the stress with lighthearted escapades. I am grateful to my friends for their support and helping to make graduate school bearable. I would like to thank Seth Boren for his wonderful positive attitude and never ceasing emotional support.

I would like to thank the undergraduate researchers who have been great collaborators: Julianna Grillot, Zayne Derden, and Rebecca Moffett. Lastly, I would like to thank my brothers in Alpha Chi Sigma, for their true and lasting friendship.

Research was supported partially through the Arkansas Biosciences Institute, the major research component of the Arkansas Tobacco Settlement Proceeds Act of 2000.

Dedication

This dissertation is dedicated to my grandmother Patricia Patrick, whose greatest dream in life was to see her grandchildren achieve the college education that she wanted to have. I wish she could be here to see how much I have accomplished, and hope that I made her proud.

Table of Contents

Table of Figures

List of Published Papers

- Chapter 3: Long-term Drifts in Sensitivity Caused by Biofouling of an Amperometric Oxygen Sensor
    - M. M. Patrick, J. M. Grillot, Z. M. Derden, D. W. Paul, *Electroanalysis* **2017**, *29*, 998.
- Chapter 4: Evaluation of PoPD on microelectrodes for oxygen sensitivity response in the presence of biofoulants and in situ calibration of biofouled oxygen sensor using generation-detection of oxygen
    - Patrick, M. M.; Halder, N.; Moffett, R. L.; Paul, D. W. "In situ recalibration of a biofouled PoPD-coated oxygen sensor using generation-detection of oxygen on a microelectrode array." Submitted to *Sensors and Actuators: B Chemical* with manuscript ID SNB-D-17-01158 (in revision).

1. Introduction to Oxygen Sensors

1.1 Introduction

Oxygen plays a vital role in many biological processes, and research has focused on developing methods of quantifying dissolved oxygen content. For example, the development of a reliable and minimally invasive oxygen sensor would be beneficial towards the diagnosis and treatment of ischemic stroke victims. Electrochemical oxygen probes function by measuring the diffusion-limited current of the dissolved oxygen content, which is directly proportional to concentration. Current electrochemical oxygen probes include the Licox probe: a small metal electrode covered by an oxygen-permeable membrane, with an internal electrolyte solution, and is the only oxygen probe approved for use in humans. An overlooked problem with traditional electrochemical oxygen probes is that the probe's in vitro calibrated sensitivity value is assumed to match that for the in vivo environment. In fact, common amongst in vivo implanted sensors is the susceptibility to adsorption of macromolecules, diminishing the sensitivity. This problem is partially solved by applying a protective membrane to the sensor. Furthermore, in vivo recalibration is not possible for oxygen sensors as is the case for glucose sensors.

1.1.1 Electrochemistry of Oxygen

The most practical and applied oxygen sensor is the design first proposed by Clark consisting of a noble metal electrode and a gas-permeable membrane separated by electrolyte solution.[1] Oxygen permeates the membrane and diffuses through the electrolyte solution before reducing at the noble metal cathode, thereby producing a concentration-dependent current response. A sufficiently negative potential is applied to the cathode in order to reduce oxygen and produce a diffusion-limited current response. The oxygen reduction mechanism at the cathode can be summarized by:

$$O_2 + 2H^+ + 2e^- \rightarrow H_2O_2;\ E^0 = +0.695V \quad \text{(Reaction 1)}$$

$$O_2 + 4H^+ + 4e^- \rightarrow 2H_2O;\ E^0 = +1.229\ V \quad \text{(Reaction 2)}$$

However, on noble metal cathodes, the reduction of oxygen occurs negative of these potential values. It has been suggested that this potential shift is due to an adsorbed oxygen film on the noble metal surface, especially for the case of the platinum electrode. It has been noted that the gold electrode may not suffer from these adsorption effects (or very minutely) as evidenced by the reduction of oxygen not being as hindered as it is for Pt, likely because the interaction between oxygen and Au is weak.[2-3] Electron transfer kinetics limit the rate of oxygen reduction at the cathode, except in the case at extremely negative potentials, in which the rate is diffusion-limited. H_2O_2 intermediate formation (Reaction 1) occurs at -0.4V vs Ag/AgCl; at more negative applied potentials (-0.8V vs Ag/AgCl), Reaction 2 dominates. Whether or not peroxide is formed is dependent upon both the applied potential and the cathode material itself.[4] For most practical purposes, Reaction 2 is used for Clark-type electrodes.

1.1.2 Biofouling

Biofouling is the adsorption of macromolecules such as proteins and cells onto the surface in the implanted probe. Due to the body's immune response, the adsorption of molecules to the probe's surface occurs within seconds to hours, followed by cell interrogation by macrophages, a possible attempt at phagocytosis, and eventual encapsulation of the implanted probe (~2 weeks).[5,6] Encapsulation would result in the implanted probe becoming isolated from the bulk tissue, meaning that the sensor would only detect the analyte in the sectioned off region in which it was confined. The biofouling resulting from implanting a probe in vivo impairs the probe's ability to function.

The main components of blood plasma and therefore likely contributors to biofouling include serum albumin and fibrinogen.[7,8] Albumins function to regulate osmotic pressure of plasma by stabilizing the extracellular fluid volume, and also to transport small biomolecules such as lipids and steroids in the blood.[9] Serum albumin is a dominant blood protein. Serum albumin (Bovine serum albumin (BSA)) undergoes reversible adsorption depending upon what surface it is exposed to.[10] The protein sequence and secondary structure of BSA was first proposed by Brown: composed of three domains, over which there are nine sulfide loops.[11] The three dimensional structure was more difficult to obtain, and at physiological pH is known to be a heart-shaped protein an equilateral triangle with sides of 80 Å and 30 Å deep. Compared to other proteins it is difficult to denature (80 ^{o}C) and changes structure with pH. Most interestingly these conformational changes are reversible. The protein presents itself as negatively charged, and the distribution of charge is evenly distributed over the surface.[12] Albumin is readily adsorbed to surfaces but can be displaced by other proteins. Both BSA and fibrinogen are known to adsorb onto gold.[13-16] BSA is a globular protein of approximately 66 kDa M.W.; fibrinogen is considerably larger at approximately 340 kDa, so one would expect fibrinogen to be a more robust foulant than BSA.[17] Fibrinogen is a cell adhesive protein that is a major component in blood coagulation, and the third most prevalent protein in plasma with a concentration of 2.6-3.0 mg/mL.[18] Fibrinogen is a "sticky," high molecular weight protein that adsorbs to both hydrophilic and hydrophobic surfaces.[19] For its size it has a low charge density but shows separate regions of positive and negative charge. At pH 7.4, the uncompensated charge per fibrinogen molecule is -7.6 from the Lorenz-Stokes relationship, which could explain the substantial adsorption onto neutral and positively charged surfaces.[18] In addition, it has been shown that near the isoelectric point (5.8), fibrinogen adsorbs in multilayers due to the strong

lateral interactions and close packing, while at much higher and lower pH (>9 and <4), monolayers of fibrinogen are observed.[18 19]

1.1.3 Polymer coatings on sensors

Using a protective film over the sensor's surface aids in diminishing biofouling effects, leading to a more stable and reliable sensor. In particular, polymer film coating holds the most promise in terms of long-term stability, coating thickness, and coating uniformity across the sensor surface. In addition, the use of polymer coatings allows for the incorporation of enzymes into the polymer matrix, thereby creating an enzyme-selective electrode; the most well-known of these enzyme-selective electrodes is the glucose sensor made by incorporating glucose oxidase into the polymer matrix. Many polymer coatings, such as Nafion coatings, have involved evaporative deposition, or dip coating. Electrochemical deposition, or electropolymerization, has the advantage over dip coating of selectively coating only the electrode surface, whereas dip coating will apply the polymer to the entire surface with which it comes into contact. With electropolymerization, multiple polymer coatings can be evaluated individually on microelectrode arrays (MEA). For example, one could study polyeugenol on one individually addressable electrode of a MEA, and polyaniline on a separate individually addressable electrode on the same MEA, without having to remove the sensor from the in vivo probe environment.

Nafion has been a popular choice for polymer coatings. It has found uses in a wide range of applications, such as fuel cells, ion-selective and biosensors, and acid catalysis.[20,21] Nafion employs electrostatic repulsion to selectively inhibit interferents from reaching the electrode surface. Nafion is generally successful at blocking negatively-charged electroactive interferents but tends to concentrate positively-charged species at the membrane surface, which can interfere with the analyte signal. Nafion is also susceptible to forming fractures in the membrane coating

if not stored in an aqueous medium, which would consequently allow interferents to pass through the membrane and contact the electrode surface.[22] Nafion employs an evaporative deposition technique to polymerize onto surfaces, which is not applicable to the current research project.

Electropolymerized polymers are of primary interest for this project, including polyeugenol (PE) and poly(o-phenylenediamine) (PoPD). PE is a non-conducting, porous polymer that allows dissolved gases (such as O_2) to diffuse readily across the membrane to the electrode while excluding larger molecules.[23] Analyte response over PE-coated glassy carbon electrodes were found to have a high permeability to the target analytes (such as nitric oxide) compared to other polymer coatings (i.e. polyaniline and polypyrrole).[24] It has also been used over graphite electrodes and shown to suppress the ascorbic acid response while enhancing the dopamine response, suggesting PE as a polymer of interest for in vivo sensors.[25] PE has also been studied over gold disk electrodes and shown to have a good permeability to oxygen while producing a stable oxygen calibration when exposed to a biofouling environment.[26] PE's lack of conductivity has the advantage over conducting polymers which have high background current that masks an analyte's signal at low concentrations. In this work, PE has been shown in preliminary data to have good oxygen permeability when electropolymerized on the MEA; however, it has also been shown to be stable for only 1-2 days, which is not applicable to longer-term in vivo studies (>2 weeks).

PoPD has been used as a protective coating in various applications, such as biosensors, metals, and electronic devices.[27,28] PoPD has been shown to be permeable to small molecules, namely hydrogen peroxide, but shows relatively low permeability to larger interferents.[29] PoPD has been used extensively in enzyme sensors such as glucose sensors, suggesting that it is permeable to oxygen, as the (first generation) glucose oxidase enzyme requires oxygen to

function.[30,31] PoPD is also thought to be one of the polymer coatings most likely to withstand long-term in vivo use.[32] PoPD's permeability to small molecules and long-term stability make it a good polymer to investigate for this current project.

1.1.4 Polymer characterization

Characterization of the polymer films is accomplished through various techniques. The use of probe molecules has been previously shown to be a viable method of characterizing uniformity and completeness of film coatings.[26] Probe molecules such as $K_3Fe(CN)_6$ and $Ru(NH_3)_6Cl_3$ function to receive electrons from the bare (uncoated) electrode surface, thereby resulting in a current response signal characteristic of the probe molecule, and indicating if the polymer coating is nonuniform. Probe molecules are ineffective to adequately characterize electrode coatings of conducting polymers because the polymer will transfer electrons through the membrane directly to the probe molecule, and thereby generating a current response. This technique was used here for the characterization of polymer coating evenness, uniformity, and degradation.

1.1.5 In situ recalibration theory

External methods of calibration require removal of the probe from the test environment. By introducing a second, oxygen-generating electrode (GE) external to the polymer membrane working electrode (WE), oxygen can be generated and the new sensitivity determined. This method is an adaptation of previously published work using 2 mm gold electrodes;[33] the innovation in this work was utilizing microelectrode arrays, and PoPD as the protective polymer coating on the working electrode. The theory of the in situ recalibration involves measuring the change in current at the detector electrode (Δi_{DL}) and current at the generator electrode (i_{GE}) and

determining "ξ," a parameter similar to collection efficiency. After fouling, the new sensitivity (S_2) can be determined using Equation (1):[33]

$$\frac{\Delta i_{DL}}{i_{GE}} = \frac{S_2}{\xi} \qquad \text{(Equation 1)}$$

By utilizing this in situ recalibration method, the oxygen sensor's change in sensitivity can be accounted for and corrected. However, the in situ calibration technique is not a magic solution that can correct for the most drastically fouled electrodes; it has its limitations just like any other technique. It is therefore first necessary to quantitate the sensitivity losses with extreme fouling, and test the maximum limit of fouling that the in situ calibration can recalibrate.

1.2 Significance

The objective of this research project is to develop a better understanding of biofouling and to contribute to knowledge of the field of in vivo oxygen sensors. The purpose of these studies is to quantify the sensitivity changes caused by biofouling of a membrane-coated oxygen sensor. Biofouling decreases the sensor's sensitivity thereby inhibiting accurate O_2 concentration readings. To attempt to minimize biofouling, a protective polymer is applied to the surface of the gold electrode via electropolymerization. Presently there are no means to recalibrate an in vivo oxygen sensor. One purpose of this project is to develop an in situ recalibration method for biofouled sensors. These projects accomplish successful application and characterization of protective polymer membranes, development of a systematic method for studying changes in sensitivity of implanted devices, and an in-depth discovery of the key components that contribute to biofouling, as well as a method for recalibration of biofouled oxygen sensors in situ. These advances could lead to improvements in oxygen sensors used in clinical applications.

1.3 Overview of the Studies Described in this Dissertation

Chapter 2 demonstrates the fundamental study of electropolymerized polymer on gold microband arrays for oxygen sensing. In this study, polyeugenol was electropolymerized onto gold microelectrode arrays and used for oxygen sensing. However, due to polymer instability, PE was not a viable option for application to in vivo sensors.

Because polyeugenol was not applicable to long-term in vivo devices, a new polymer (PoPD) was investigated in Chapter 3. These experiments utilized 2 mm gold disc macroelectrodes in order to understand the behavior of PoPD on gold electrodes for oxygen sensing in the presence of biofoulants: BSA, fibrinogen, and rat brain homogenate. This study also simulated the in vivo recalibration practices typically used in the field of in vivo sensors, proving the extent of the problems associated with these current practices.

Chapter 4 focuses on application of PoPD to microelectrode arrays for oxygen sensing in the presence of biofoulants: BSA, fibrinogen, and blood serum. These experiments also include a generation-detection of oxygen scheme, which can be used to predict a new sensor sensitivity when the sensor is biofouled and has a subsequent sensitivity change.

Each chapter in this dissertation is written in a format that is compatible for publication in peer-reviewed scientific journals.

1.4 References

1. Clark, L. C., Jr.; Wold, R.; Granger, D.; Taylor, Z., Continuous recording of blood oxygen tensions by polarography. *Journal of Applied Physiology (1948-1976)* **1953,** *6*, 189-93.

2. Rao, M. L. B.; Damjanovic, A.; Bockris, J. O. M., Oxygen adsorption related to the unpaired d-electrons in transition metals. *Journal of Physical Chemistry* **1963,** *67* (11), 2508-9.

3. Hoare, J. P., Oxygen [electrochemistry]. *Encycl. Electrochem. Elem.* **1974,** *2*, 191-382.

4. Hoare, J. P., *The electrochemistry of oxygen*. Interscience Publishers: New York,, 1968; p xiv, 423 p.

5. Ratner, B. D.; Bryant, S. J., Biomaterials: Where we have been and where we are going. *Annual Review of Biomedical Engineering* **2004,** *6*, 41-75.

6. Anderson, J. M.; Rodriguez, A.; Chang, D. T., Foreign body reaction to biomaterials. *Semin. Immunol.* **2008,** *20* (2), 86-100.

7. Riedel, T.; Riedelova-Reicheltova, Z.; Majek, P.; Rodriguez-Emmenegger, C.; Houska, M.; Dyr, J. E.; Brynda, E., Complete Identification of Proteins Responsible for Human Blood Plasma Fouling on Poly(ethylene glycol)-Based Surfaces. *Langmuir* **2013,** *29* (10), 3388-3397.

8. Gunkel, G.; Huck, W. T. S., Cooperative Adsorption of Lipoprotein Phospholipids, Triglycerides, and Cholesteryl Esters Are a Key Factor in Nonspecific Adsorption from Blood Plasma to Antifouling Polymer Surfaces. *Journal of the American Chemical Society* **2013,** *135* (18), 7047-7052.

9. Ha, C.-E.; Bhagavan, N. V., Novel insights into the pleiotropic effects of human serum albumin in health and disease. *Biochimica et Biophysica Acta, General Subjects* **2013,** *1830* (12), 5486-5493.

10. Carter, D. C.; Ho, J. X., Structure of serum albumin. *Advances in Protein Chemistry* **1994,** *45* (LIPOPROTEINS,APOLIPOPROTEINS, AND LIPASES), 153-203.

11. Brown, J. R., Serum albumin: amino acid sequence. In *Albumin Structure, Function, and Uses*, Rosenoer, V. M.; Oratz, M.; Rotschild, M. A., Eds. Pergamon Press: Oxford, 1977; pp 27-51.

12. Peters, T., Jr., Serum albumin. *Adv. Protein Chem.* **1985,** *37*, 161-245.

13. Nelson, D. L.; Cox, M. M., *Lehninger: Principles of Biochemistry*. 4th ed.; W. H. Freeman and Company: New York, NY, 2008.

14. Moulton, S. E.; Barisci, J. N.; Bath, A.; Stella, R.; Wallace, G. G., Investigation of protein adsorption and electrochemical behavior at a gold electrode. *Journal of Colloid and Interface Science* **2003,** *261* (2), 312-319.

15. Moulton, S. E.; Barisci, J. N.; Bath, A.; Stella, R.; Wallace, G. G., Studies of double layer capacitance and electron transfer at a gold electrode exposed to protein solutions. *Electrochimica Acta* **2004,** *49* (24), 4223-4230.

16. Ying, P.; Viana, A. S.; Abrantes, L. M.; Jin, G., Adsorption of human serum albumin onto gold: a combined electrochemical and ellipsometric study. *Journal of Colloid and Interface Science* **2004,** *279* (1), 95-99.

17. Glomm, W. R.; Halskau, O., Jr.; Hanneseth, A.-M. D.; Volden, S., Adsorption Behavior of Acidic and Basic Proteins onto Citrate-Coated Au Surfaces Correlated to Their Native Fold, Stability, and pI. *Journal of Physical Chemistry B* **2007,** *111* (51), 14329-14345.

18. Wasilewska, M.; Adamczyk, Z.; Jachimska, B., Structure of Fibrinogen in Electrolyte Solutions Derived from Dynamic Light Scattering (DLS) and Viscosity Measurements. *Langmuir* **2009,** *25* (6), 3698-3704.

19. Feng, L.; Andrade, J. D., Structure and adsorption properties of fibrinogen. *ACS Symposium Series* **1995,** *602* (Proteins at Interfaces 2), 66-79.

20. Heitner-Wirguin, C., Recent advances in perfluorinated ionomer membranes: structure, properties and applications. *Journal of Membrane Science* **1996,** *120* (1), 1-33.

21. Gelbard, G., Organic synthesis by catalysis with ion-exchange resins. *Industrial & Engineering Chemistry Research* **2005,** *44* (23), 8468-8498.

22. Njagi, J. I.; Kagwanja, S. M., The interface in biosensing: improving selectivity and sensitivity. *ACS Symposium Series* **2011,** *1062* (Interfaces and Interphases in Analytical Chemistry), 225-247, 5 plates.

23. Borgmann, S., Electrochemical quantification of reactive oxygen and nitrogen: challenges and opportunities. *Analytical and Bioanalytical Chemistry* **2009,** *394* (1), 95-105.

24. Ciszewski, A.; Milczarek, G., A new Nafion-free bipolymeric sensor for selective and sensitive detection of nitric oxide. *Electroanalysis* **1998,** *10* (11), 791-793.

25. Hirakawa, K.; Imato, T.; Yamasaki, S.; Ohura, H., Electrochemical responses of a polyeugenol and overoxidized polypyrrole composite film modified graphite electrode to dopamine and ascorbic acid. *Proceedings - Electrochemical Society* **2004,** *2004-08* (Chemical Sensors VI), 438-443.

26. Paul, D. W.; Prajapati, I.; Reed, M. L., Electropolymerized eugenol: Evaluation as a protective film for oxygen sensing. *Sensors and Actuators, B: Chemical* **2013,** *183*, 129-135.

27. Long, J. W.; Rhodes, C. P.; Young, A. L.; Rolison, D. R., Ultrathin, Protective Coatings of Poly(o-phenylenediamine) as Electrochemical Proton Gates: Making Mesoporous MnO2 Nanoarchitectures Stable in Acid Electrolytes. *Nano Lett.* **2003,** *3* (8), 1155-1161.

28. Chirizzi, D.; Malitesta, C., Potentiometric urea biosensor based on urease immobilized by an electrosynthesized poly(o-phenylenediamine) film with buffering capability. *Sens. Actuators, B* **2011,** *157* (1), 211-215.

29. Dai, Y.-Q.; Zhou, D.-M.; Shiu, K.-K., Permeability and permselectivity of polyphenylenediamine films synthesized at a palladium disk electrode. *Electrochimica Acta* **2006,** *52* (1), 297-303.

30. Rothwell, S. A.; Killoran, S. J.; O'Neill, R. D., Enzyme immobilization strategies and electropolymerization conditions to control sensitivity and selectivity parameters of a polymer-enzyme composite glucose biosensor. *Sensors* **2010,** *10*, 6439-6462.

31. Lowry, J. P.; McAteer, K.; El Atrash, S. S.; Duff, A.; O'Neill, R. D., Characterization of Glucose Oxidase-Modified Poly(phenylenediamine)-Coated Electrodes in vitro and in vivo: Homogeneous Interference by Ascorbic Acid in Hydrogen Peroxide Detection. *Anal. Chem.* **1994,** *66* (10), 1754-61.

32. Killoran, S. J.; O'Neill, R. D., Characterization of permselective coatings electrosynthesized on Pt-Ir from the three phenylenediamine isomers for biosensor applications. *Electrochimica Acta* **2008,** *53* (24), 7303-7312.

33. Johnson, C. D.; Paul, D. W., In situ calibrated oxygen electrode. *Sens. Actuators, B* **2005,** *105* (2), 322-328.

2. Evaluation of Eugenol on Microelectrodes for Long-Term Stability, Coating Uniformity, and Oxygen Sensitivity Response

2.1 Abstract

Polyeugenol (PE) has been shown in previous work to be permeable to oxygen and effectively protect the oxygen electrode from biofouling using gold macroelectrodes. This work investigated PE as a possible protective polymer membrane coating for use with microelectrodes, as they are more applicable towards in vivo applications. These data show effective polymer adhesion to a gold microelectrode on a microelectrode array, PE's permeability to oxygen via calibration curves, and effective blocking of the probe molecule ferricyanide. These data also show PE degradation on the gold microelectrode, rendering it impractical towards future in vivo applications.

2.2 Introduction

Eugenol is the primary component of clove oil derived via hydrodistillation of *Eugenia caryphyllata* buds and leaves.[1] Eugenol has been studied extensively for its wide uses in a variety of fields, such as pharmaceutics, agriculture, and cosmetic industries. It has been of particular interest for medicinal uses as an antibacterial, antifungal, anti-inflammatory,[2-4] analgesic, anti-oxidant,[2, 5] and anticancer activities; it has also been studied as an antifumagant and repellant,[6] anticarcinogen,[7] anticonvulsant,[8] and antimutagen.[9]

Eugenol is an allyl chain-substituted guaiacol (Figure 2.1) that is weakly acidic, slightly soluble in water, and soluble in organic solvents; it is a pale to yellow liquid with a distinct clove smell and spicy taste.[1] Eugenol can be produced synthetically via the allylation of guaiacol with allyl chloride.[1] It is thought to have antimicrobial, chemopreventive effects, and antioxidant activity due to the phenolic group.[10]

The combination of eugenol with conventional antibiotics is thought to have synergistic effects. Hemaiswarya et al noted that 1 mM eugenol damaged nearly 50% of the Gram-negative bacterial membrane, which allowed increased penetration of vancomycin and β-lactam antibiotics and therefore an increased microbial effect.[11] Eugenol combined with ampicillin and gentamicin exhibited a higher kill rate of bacteria over 60 minutes than with antibiotics alone.[12] Significant synergistic effects against *Escherichia coli* were noted when eugenol was combined with cinnamaldehyde, thymol, carvacrol, and their combinations, even though eugenol itself has the lowest antibacterial activity on its own.[13]

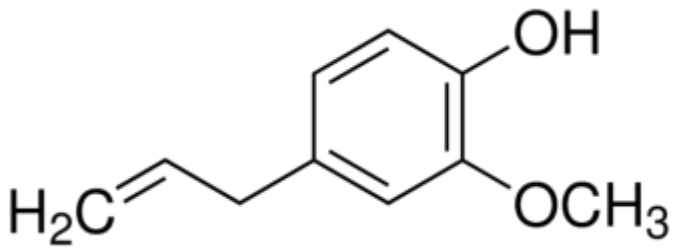

Figure 2.1 Molecular structure of eugenol monomer. Image obtained from MP Bio, http://www.mpbio.com/product.php?pid=02151106&country=223 (accessed April 7, 2017).

The mechanism of eugenol's apparent synergistic effect is proposed to be due to the induced cell lysis causing leakage of proteins and lipid contents, as well as damage to both cell wall and membrane of Gram-negative and Gram-positive bacteria.[14] In addition, eugenol could be added to food products as an antimicrobial agent in order to suppress the production of exotoxins by *S. aureus*.[15]

Eugenol has exhibited antifungal properties against a wide variety of species.[16-18] Eugenol has an even more potent activity than some known synthetic antimicrobial compounds and is applicable to a wide spectrum of *Aspergillus* species.[19] Eugenol is lipophilic, and can therefore easily get between acyl chains of the cell membrane to modify the permeability of cell membranes and disturb cell growth.[20-21] Eugenol has proven to be highly toxic to *C. albicans*, affecting the membrane integrity and causing arrest of the cell cycle, thereby killing 99.9% within 7 minutes following exposure.[22] In addition, eugenol was used prophylactically and as a treatment for experimental vaginal candidiasis with immunosuppressed rats; results show that after 10 days of inoculation, eugenol reduced the number of colonies of *C. albicans* by 98.9%.[23] Eugenol also shows an antifungal synergistic effect. Eugenol and methyleugenol were tested with fluconazole (an antifungal drug) against various fluconazole-sensitive and fluconazole-resistant *C. albicans* strains, which resulted in all strains exhibiting susceptibility; these results suggest that eugenol/methyleugenol could be used in combination with traditional antifungal as an alternative treatment.[24-25]

Eugenol has been used extensively as an analgesic for dental, antinociceptive, and anesthetic applications. Eugenol (in doses of 50, 75, and 100 mg/kg) was evaluated as an oral analgesic for mice via the acetic acid-induced abdominal writhing method; eugenol was shown to have a significant effect over a period of 30 minutes in a dose-dependent manner on the

reduction of pain as measured by the number of contractions of the body.[3, 26] Lee et al noted that eugenol inhibited high-voltage-activated Ca^{2+} channel (HVACC) currents in dental primary afferent neurons, which are composed of primarily pain neurons; these results suggest that HVACC inhibition may play a role in eugenol's apparent analgesic properties.[27] Eugenol has also been studied as an anesthetic using various fish models; results found that eugenol has a strong anesthetic effect[28-31], but sometimes with slow recovery.[31]

New methods for treating or preventing cancer is a widely studied and necessary field of research interest. Specifically, focus has been on compounds derived from natural sources, to replace conventional anticancer treatments that often have harmful side effects. Eugenol has been studied alone and in conjunction with a conventional chemotherapeutic drug (gemcitabine) against HeLa cells (an immortal cell line derived from Henrietta Lacks's cervical cancer cells); eugenol showed a dose-dependent selective cytotoxicity to the HeLa cells as compared to normal cells, and the combination treatment of eugenol (150 μM) and gemcitabine (15 μM) decreased HeLa cell viability to 47%, an improvement over eugenol alone (84%) and gemcitabine alone (51%).[18] Eugenol also induced apoptosis of colon cancer cells, increasing the lipid layer break and reducing the intracellular non-protein thiols.[32] Eugenol was an effective inhibitor of melanoma cell proliferations, delaying tumor growth and effecting a 40% decrease in tumor size; it also seemed to impact metastasis, as 50% of the control group died due to metastasis, while zero in the treatment group were affected by metastasis.[33]

A mechanism for polymerization has been proposed and is similar to those described for oxidative polymerization of porphyrins,[34] vanillin,[35] guaiacol,[36] and epidotoxin.[37] Eugenol monomer is polymerized to polyeugenol (PE) via oxidative polymerization though the hydroxyl group in alkaline solution.[38-39] In alkaline solution, the phenol group exists as the phenolate ion

(I) (Fig. 2.2) which is readily oxidized via a one-electron transfer to generate a free radical (II).[38] Then, interacting with a methoxy group on a monomer molecule, methanol is eliminated via alkaline hydrolysis and generates an anion radical (III) which is then converted via a one-electron reaction to o-quinone (IV).[38] The mechanism for polymer growth on the electrode surface is less clear. Possible mechanisms include: a free radical step-growth polymerization initiated by (II);[40] a Diels-Alder reaction between o-quinone (IV) and allyl C=C bound giving a 1,4-benzenedioxane subunit;[41] dimerization of radical (II);[42] creation of lignan-like subunits by oxidative coupling of substrate molecules;[42-43] or hydroxylation of (IV) leading to p-quinone.[38, 44]

Polyeugenol is a non-conducting, porous polymer that allows dissolved gases (such as O_2) to diffuse readily across the membrane to the electrode while excluding larger molecules.[45] PE has been applied to sensors for a variety of applications. PE has been applied to platinum,[39, 46-48] glassy carbon,[46] and carbon fiber microdisk[48] electrodes for nitric oxide sensing. PE has also been utilized for dopamine detection,[38, 49] and retained 85% of the initial dopamine response after 10 days.[38] Although PE has been used in detection of larger molecules,[50] nitric oxide sensor applications show PE's permeability to small molecules and therefore possible applications to oxygen sensors. PE's lack of conductivity has the advantage over conducting polymers with high background current that could mask an analyte's signal at low concentrations. PE films are typically used for analytes detected via oxidation, but not used in many studies utilizing negative potentials.[47] Paul et al were successful in studying PE over gold macrodisk electrodes; the electrodes were shown to have a good permeability to oxygen while producing a stable oxygen calibration when exposed to a biofouling environment.[51] PE showed great promise for applications to microelectrode array oxygen sensor, but a stability study had not been done

previously; this work includes a stability study of PE-coated MEA for oxygen sensing, to a disappointing conclusion.

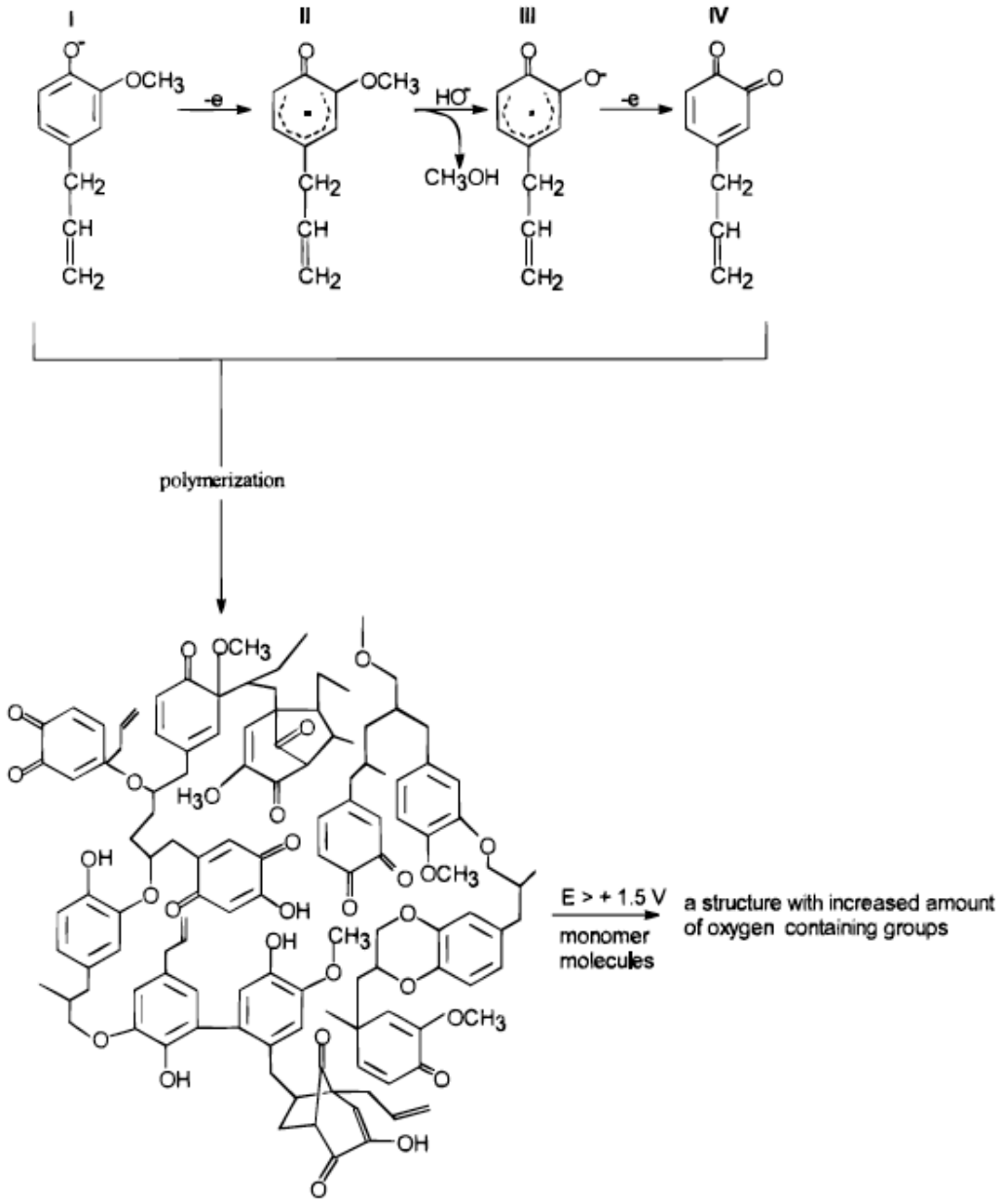

Figure 2.2 Proposed mechanism for eugenol polymerization. Image obtained from: Ciszewski, A.; Milczarek, G., Polyeugenol-modified platinum electrode for selective detection of dopamine in the presence of ascorbic acid. Anal. Chem. 1999, 71 (5), 1055-1061.[38]

2.3 Materials and Methods

2.3.1 Reagents

NaCl (VWR), KCl and $NaHCO_3$ (EMD), $CaCl_2$ (Amresco), D-glucose (Alfa Aesar), $MgCl_2$ and NaH_2PO_4 (Sigma-Aldrich) were obtained and used as received. The aCSF solution was prepared using the following concentrations of components: 119 mM NaCl, 2.5 mM KCl, 1.3 mM $MgCl_2$, 2.5 mM $CaCl_2$, 1 mM NaH_2PO_4, 26.2 mM $NaHCO_3$, and 10 mM D-glucose.[52] Eugenol monomer (99%) was obtained from Alfa Aesar and used as received without further purification. Unless otherwise stated, a Ag/AgCl in sat'd KCl reference electrode was used in all experiments.

2.3.2 Working electrode preparation

Microelectrodes used in the study consisted of an array of sixteen interdigitated microbands (2 mm long, 25 µm width and 25 µm gap) on a 1 in x 1 in silicon substrate; an insulating layer of benzocyclobutane (BCB) covered the entire chip except the exposed array and contact pads. The eugenol polymerization was accomplished on a single gold electrode of the MEA using 10 mM eugenol in 0.1 M NaOH and sweeping the potential from 0.0 V to 0.7 V at a scan rate of 100 mV/s for 40 cycles.[51]

2.3.3 Oxygen calibration curves

The current response from the oxygen cyclic voltammograms (CVs) were obtained on a CHI 830 potentiostat at -0.6 V vs Ag/AgCl in sat'd KCl reference at increasing dissolved oxygen concentrations. The dissolved oxygen concentration was measured with a YSI model 55 oxygen meter. The solutions were purged of dissolved oxygen by bubbling nitrogen through the solution. The oxygen CVs were obtained versus Ag/AgCl (in sat'd KCl) reference and platinum flag

auxiliary electrodes. The oxygen calibration curve was constructed (Fig. 2.3) by analyzing the current response from the oxygen CVs at -0.6 V.

2.3.4 Polyeugenol stability

The PE-coated electrode was compared to a bare electrode on the same array by cyclic voltammetry in 5 mM $K_3Fe(CN)_6$ in 0.1 M KCl from 0.5 V to -0.2 V vs Ag/AgCl in sat'd KCl reference using a scan rate of 100 mV/s for one cycle. The integrity of the PE coating was investigated using ferricyanide as a probe molecule to assess imperfections in the polymer layer.

2.4 Results and Discussion

The permeability of oxygen through the PE coating was investigated. An oxygen calibration curve was constructed in artificial cerebrospinal fluid (aCSF) solution to compare PE-coated and bare electrodes. The PE-coated and bare electrodes exhibited similar sensitivities confirmed by Student's t-test (0.110 ±0.004μA/ppm and 0.107±0.005 μA/ppm, respectively), suggesting that oxygen is readily permeable through the protective PE film (Fig. 2.3).

Potassium ferricyanide, $K_3Fe(CN)_6$, was used as a probe molecule to test the uniformity of the PE coating. If the ferricyanide molecule is able to contact the surface of the electrode, a typical ferricyanide signal is observed (Fig. 2.4, bare); the high magnitude of current is likely a result of the MEA chip being cleaned in RCA-1 solution prior to use, which has been shown to remove the insulating BCB layer, thereby exposing more than the 2 mm as it was designed. Nevertheless, the comparison of PE-coated and bare microelectrodes (Fig. 2.4) exhibits the loss of ferricyanide signal after polymerization, suggesting that the PE coating was complete; there is also an increase in background charging current for the PE-coated electrode (0.92 μA) due to the presence of the polymer membrane on the electrode surface. An additional CV was obtained on the PE-coated electrode 24 hours later (Fig. 2.5); these data show a ferricyanide signal after only

24 hours as can be seen by the change in shape to a more sigmoidal signal that is indicative of a ferricyanide signal. These characterization studies indicate that the PE coating degrades over time. A possible reason for why other researchers have shown PE stability over time, a direct contradiction to the findings in this study, is that previous work has not focused on using negative applied potentials;[47] the extreme negative applied potential could induce a local change in the polymer structure that is exacerbated with continued use.

Using the Randles-Sevcik equation (Eq. 2.1), a total electrode surface area of 1.22E-2 cm^2 was calculated for the bare electrode in Fig. 2.4; this differs from the expected surface area of 5E-4 cm^2, assuming a 25 μm x 2 mm MEA individual electrode. This difference is due to the insulating BCB layer detaching from the chip during a cleaning procedure, leaving more of the gold finger exposed and therefore electroactive.

$$i_p = (2.69\times10^{-5})n^{3/2}AD_o^{1/2}\nu^{1/2}C_o^* \tag{2.1}$$

i_p is the peak current; n is the # of moles; A is the surface area of electrode; D_o is the diffusion coefficient; ν is the scan rate; C_o* is the concentration of electroactive species in the bulk.

In regards to Fig. 2.5, the presence of a slightly sigmoidal curve indicates microelectrode behavior and incomplete polymer coverage in which electron transfer is blocked and non-linear diffusion effects are observed;[53] this could be due to many small pores or a few large cracks in the polymer membrane. Assuming that the current response is due to the former, an average electroactive pore size was calculated to be 6.94 nm, with an average distance between pores of 70.97 nm according to the following equations derived for cases in which the electron transfer is blocked by a film that almost completely covers the electrode surface:[53]

$$2R_o(1-\theta)\not{r}(1-\theta) = \left(\frac{D}{k_{s,0}^{a,p}}\right)e^{\left[\left(\frac{\alpha F}{RT}\right)\left(E_{1/2}-E_0\right)\right]} \tag{2.2}$$

$$R_a = R_o(1-\theta)^{1/2} \tag{2.3}$$

where R_o is the distance between active sites; R_a is the size of active site; θ is the fractional coverage of the electrode; D is the diffusion coefficient; $k_{s,0}^{a,p}$ is the rate constant at an unblocked electrode (0.095 cm/s);[54-55] α is the transfer coefficient (0.55);[54-55] $E_{1/2}$ is the half-wave potential; E_0 is the standard reduction potential, and $f(1-\theta)$ assuming a disc-type active site is:[53]

$$f(1-\theta) = 0.3(1-\theta)^{1/2} \tag{2.4}$$

For this calculation, the average of i_c and i_a current at 0 V was obtained, to account for the high capacitive current for both a bare electrode (Fig. 2.4) and a PE-coated after 24 hours (Fig. 2.5), and θ was calculated to be 0.043 via:

$$\theta = \frac{i_{coated}}{i_{bare}} \tag{2.5}$$

A pore size of 6.94 nm is in good agreement with the concept that the current response is due to many small pores acting as additive microelectrodes. These calculations are approximate, as they assume a hypothetical averaged distribution in which the dimensions of actives sites and distances between them are the same.[53]

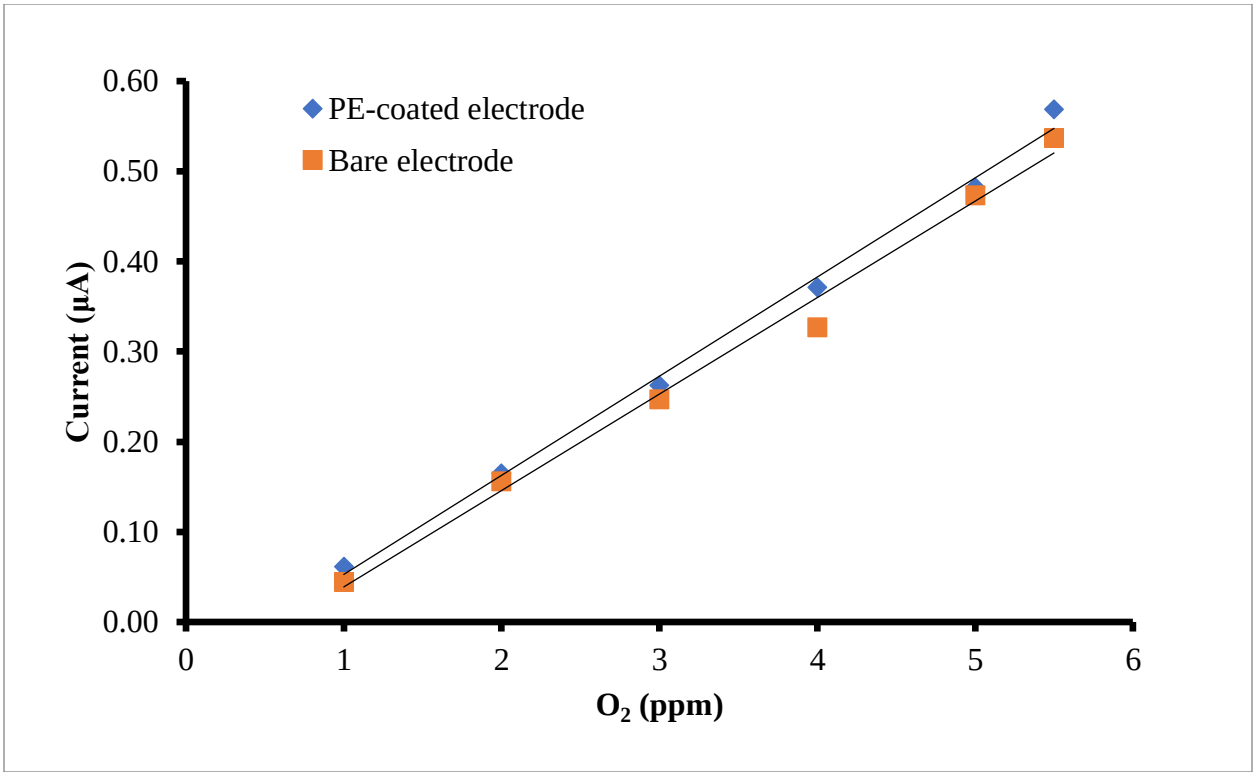

Figure 2.3 Oxygen calibration curves of PE-coated (blue diamonds) and bare (orange squares) electrodes in aCSF; Ag/AgCl in sat'd KCl reference, n=1. Bare and PE-coated electrodes exhibit the same sensitivity value within experimental uncertainty: PE-coated sensitivity of 0.110±0.004 µA/ppm, bare electrode sensitivity of 0.107±0.005 µA/ppm via line statistics function.

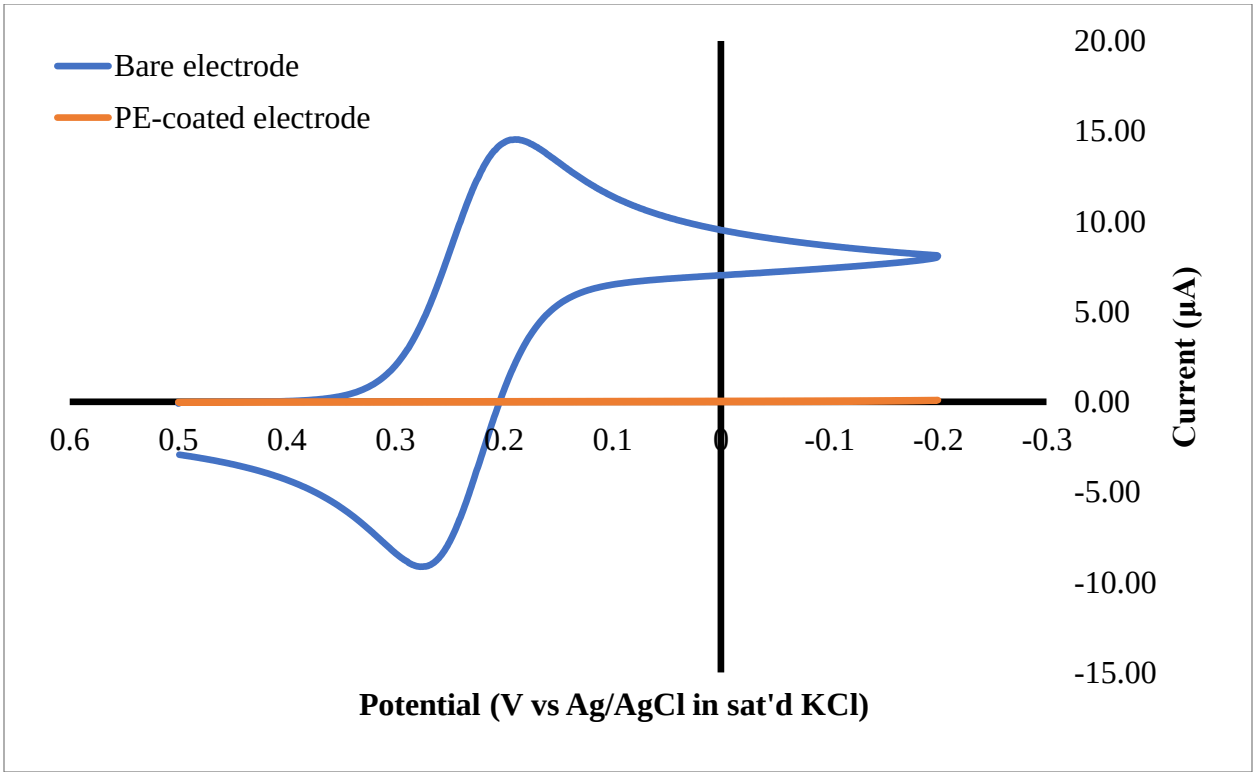

Figure 2.4 Comparison of ferricyanide signal for PE-coated and bare microelectrodes on the MEA; electroactive surface area of bare electrode: 1.22E-2 cm^2, much larger than the expected 5E-4 cm^2 for a single electrode finger. The difference is expected to be caused by loss of BCB insulation layer during a cleaning procedure.

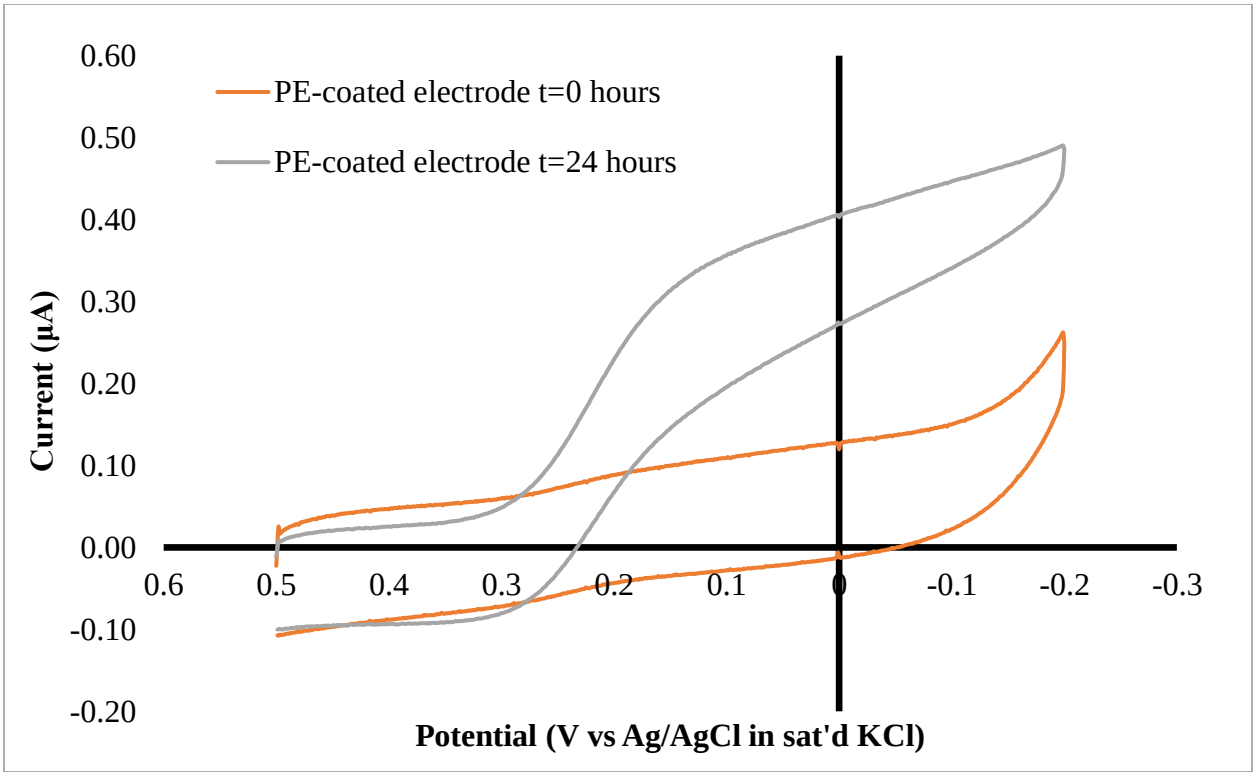

Figure 2.5 Stability study of the PE coating on a single gold electrode of the MEA; average electroactive pore size was calculated to be 6.94 nm, with an average distance between pores of 70.97 nm.

2.5 Conclusion

PE-coated and bare microelectrodes exhibited similar sensitivities to oxygen. Potassium ferricyanide, used as a probe molecule, exhibited uniform PE coating, followed by a nonuniform PE coating after 24 hours. As the PE coating was proven to be mechanically unstable, biofouling studies were not conducted on a PE-coated microelectrode. This is the first work utilizing probe molecule ferricyanide to test the uniformity of a PE coating. While the PE film did show oxygen permeability, the degradation of the film after only 1 day makes PE unsuitable for our work towards in vivo oxygen sensors.

2.6 Acknowledgements

The authors acknowledge financial support from the Arkansas Biosciences Institute, the major research component of the Arkansas Tobacco Settlement Proceeds Act of 2000. The authors are also grateful to the Fritsch group at the University of Arkansas for the donation of the MEA chip used in this study.

2.7 References

1. Kamatou, G. P.; Vermaak, I.; Viljoen, A. M., Eugenol - from the remote Maluku islands to the international market place: a review of a remarkable and versatile molecule. *Molecules* **2012,** *17*, 6953-6981.

2. Leem, H.-H.; Kim, E.-O.; Seo, M.-J.; Choi, S.-W., Antioxidant and anti-inflammatory activities of eugenol and its derivatives from clove (Eugenia caryophyllata Thunb.). *Han'guk Sikp'um Yongyang Kwahak Hoechi* **2011,** *40* (10), 1361-1370.

3. Daniel, A. N.; Sartoretto, S. M.; Schmidt, G.; Caparroz-Assef, S. M.; Bersani-Amado, C. A.; Cuman, R. K. N., Anti-inflammatory and antinociceptive activities of eugenol essential oil in experimental animal models. *Revista Brasileira de Farmacognosia* **2009,** *19* (1B), 212-217.

4. Sharma, J. N.; Srivastava, K. C.; Gan, E. K., Suppressive effects of eugenol and ginger oil on arthritic rats. *Pharmacology* **1994,** *49* (5), 314-18.

5. Chogo, J. B.; Crank, G., Chemical composition and biological activity of the Tanzanian plant Ocimum suave. *Journal of Natural Products* **1981,** *44* (3), 308-11.

6. Ogendo, J. O.; Kostyukovsky, M.; Ravid, U.; Matasyoh, J. C.; Deng, A. L.; Omolo, E. O.; Kariuki, S. T.; Shaaya, E., Bioactivity of Ocimum gratissimum L. oil and two of its constituents against five insect pests attacking stored food products. *Journal of Stored Products Research* **2008,** *44* (4), 328-334.

7. Zheng, G. Q.; Kenney, P. M.; Lam, L. K., Sesquiterpenes from clove (Eugenia caryophyllata) as potential anticarcinogenic agents. *J Nat Prod* **1992,** *55* (7), 999-1003.

8. Harborne, J. B.; Baxter, H.; Moss, G. P.; Editors, *Phytochemical Dictionary: A Handbook of Bioactive Compounds from Plants, Second Edition*. 1998; p 900 pp.

9. Miyazawa, M.; Hisama, M., Suppression of chemical mutagen-induced SOS response by alkylphenols from clove (Syzygium aromaticum) in the Salmonella typhimurium TA1535/pSK1002 umu test. *Journal of Agricultural and Food Chemistry* **2001,** *49* (8), 4019-4025.

10. Yogalakshmi, B.; Viswanathan, P.; Anuradha, C. V., Investigation of antioxidant, anti-inflammatory and DNA-protective properties of eugenol in thioacetamide-induced liver injury in rats. *Toxicology* **2010,** *268* (3), 204-212.

11. Hemaiswarya, S.; Doble, M., Synergistic interaction of eugenol with antibiotics against Gram negative bacteria. *Phytomedicine* **2009,** *16* (11), 997-1005.

12. Moon, S.-E.; Kim, H.-Y.; Cha, J.-D., Synergistic effect between clove oil and its major compounds and antibiotics against oral bacteria. *Archives of Oral Biology* **2011,** *56* (9), 907-916.

13. Pei, R.-S.; Zhou, F.; Ji, B.-P.; Xu, J., Evaluation of combined antibacterial effects of eugenol, cinnamaldehyde, thymol, and carvacrol against E. coli with an improved method. *Journal of Food Science* **2009,** *74* (7), M379-M383.

14. Oyedemi, S. O.; Okoh, A. I.; Mabinya, L. V.; Pirochenva, G.; Afolayan, A. J., The proposed mechanism of bactericidal action of eugenol, α-terpineol and γ-terpinene against Listeria monocytogenes, Streptococcus pyogenes, Proteus vulgaris and Escherichia coli. *African Journal of Biotechnology* **2009,** *8* (7), 1280-1286.

15. Qiu, J.; Feng, H.; Lu, J.; Xiang, H.; Wang, D.; Dong, J.; Wang, J.; Wang, X.; Liu, J.; Deng, X., Eugenol reduces the expression of virulence-related exoproteins in Staphylococcus aureus. *Applied and Environmental Microbiology* **2010,** *76* (17), 5846-5851.

16. Gayoso, C. W.; Lima, E. O.; Oliveira, V. T.; Pereira, F. O.; Souza, E. L.; Lima, I. O.; Navarro, D. F., Sensitivity of fungi isolated from onychomycosis to Eugenia cariophyllata essential oil and eugenol. *Fitoterapia* **2005,** *76* (2), 247-249.

17. Park, M. J.; Gwak, K. S.; Yang, I.; Kim, K. W.; Jeung, E. B.; Chang, J. W.; Choi, I. G., Effect of citral, eugenol, nerolidol and alpha-terpineol on the ultrastructural changes of Trichophyton mentagrophytes. *Fitoterapia* **2009,** *80* (5), 290-6.

18. Hussain, A.; Brahmbhatt, K.; Priyani, A.; Ahmed, M.; Rizvi, T. A.; Sharma, C., Eugenol Enhances the Chemotherapeutic Potential of Gemcitabine and Induces Anticarcinogenic and Anti-inflammatory Activity in Human Cervical Cancer Cells. *Cancer Biotherapy and Radiopharmaceuticals* **2011,** *26* (5), 519-527.

19. Kumar, A.; Shukla, R.; Singh, P.; Dubey, N. K., Biodeterioration of some herbal raw materials by storage fungi and aflatoxin and assessment of Cymbopogon flexuosus essential oil and its components as antifungal. *International Biodeterioration & Biodegradation* **2009,** *63* (6), 712-716.

20. Pina-Vaz, C.; Goncalves Rodrigues, A.; Pinto, E.; Costa-de-Oliveira, S.; Tavares, C.; Salgueiro, L.; Cavaleiro, C.; Goncalves, M. J.; Martinez-de-Oliveira, J., Antifungal activity of

Thymus oils and their major compounds. *Journal of the European Academy of Dermatology and Venereology : JEADV* **2004,** *18* (1), 73-8.

21. Sikkema, J.; de Bont, J. A.; Poolman, B., Mechanisms of membrane toxicity of hydrocarbons. *Microbiol Rev* **1995,** *59* (2), 201-22.

22. Zore, G. B.; Thakre, A. D.; Jadhav, S.; Karuppayil, S. M., Terpenoids inhibit Candida albicans growth by affecting membrane integrity and arrest of cell cycle. *Phytomedicine* **2011,** *18* (13), 1181-1190.

23. Chami, F.; Chami, N.; Bennis, S.; Trouillas, J.; Remmal, A., Evaluation of carvacrol and eugenol as prophylaxis and treatment of vaginal candidiasis in an immunosuppressed rat model. *Journal of Antimicrobial Chemotherapy* **2004,** *54* (5), 909-914.

24. Ahmad, A.; Khan, A.; Khan, L. A.; Manzoor, N., In vitro synergy of eugenol and methyleugenol with fluconazole against clinical Candida isolates. *Journal of Medical Microbiology* **2010,** *59* (10), 1178-1184.

25. Khan, M. S. A.; Malik, A.; Ahmad, I., Anti-candidal activity of essential oils alone and in combination with amphotericin B or fluconazole against multi-drug resistant isolates of Candida albicans. *Medical Mycology* **2012,** *50* (1), 33-42.

26. Park, S.-H.; Sim, Y.-B.; Lee, J.-K.; Kim, S.-M.; Kang, Y.-J.; Jung, J.-S.; Suh, H.-W., The analgesic effects and mechanisms of orally administered eugenol. *Archives of Pharmacal Research* **2011,** *34* (3), 501-507.

27. Lee, M. H.; Yeon, K. Y.; Park, C. K.; Li, H. Y.; Fang, Z.; Kim, M. S.; Choi, S. Y.; Lee, S. J.; Lee, S.; Park, K.; Lee, J. H.; Kim, J. S.; Oh, S. B., Eugenol inhibits calcium currents in dental afferent neurons. *Journal of Dental Research* **2005,** *84* (9), 848-851.

28. Vidal, L. V. O.; Furuya, W. M.; Graciano, T. S.; Schamber, C. R.; dos Santos, L. D.; Soares, C. M., Eugenol concentrations for deep anesthesia and acute toxicity in piavucu (Leporinus macrocephalus) juveniles. *Acta Scientiarum, Biological Sciences* **2007,** *29* (4), 357-362.

29. Okamoto, M. H.; Tesser, M. B.; Louzada, L. R.; Adriano dos Santos, R.; Sampaio, L. A., Benzocaine and eugenol as anesthetics for pompano juvenile Trachinotus marginatus. *Ciencia Rural* **2009,** *39* (3), 866-870.

30. Parodi, T. V.; Cunha, M. A.; Heldwein, C. G.; de Souza, D. M.; Martins, A. C.; Garcia, L. d. O.; Wasielesky, W., Jr.; Monserrat, J. M.; Schmidt, D.; Caron, B. O.; Heinzmann, B.; Baldisserotto, B., The anesthetic efficacy of eugenol and the essential oils of Lippia alba and Aloysia triphylla in post-larvae and sub-adults of Litopenaeus vannamei (Crustacea, Penaeidae). *Comparative Biochemistry and Physiology, Part C: Toxicology & Pharmacology* **2012,** *155* (3), 462-468.

31. Filiciotto, F.; Buscaino, G.; Buffa, G.; Bellante, A.; Maccarrone, V.; Mazzola, S., Anaesthetic qualities of eugenol and 2-phenoxyethanol and their effect on same haematological parameters in farmed European sea bass (Dicentrarchus labrax L.). *Journal of Animal and Veterinary Advances* **2012,** *11* (4), 494-502, 9 pp.

32. Jaganathan, S. K.; Mazumdar, A.; Mondhe, D.; Mandal, M., Apoptotic effect of eugenol in human colon cancer cell lines. *Cell Biology International* **2011,** *35* (6), 607-615.

33. Ghosh, R.; Ganapathy, M.; Alworth, W. L.; Chan, D. C.; Kumar, A. P., Combination of 2-methoxyestradiol (2-ME2) and eugenol for apoptosis induction synergistically in androgen independent prostate cancer cells. *Journal of Steroid Biochemistry and Molecular Biology* **2009,** *113* (1-2), 25-35.

34. Malinski, T.; Ciszewski, A.; Bennett, J.; Fish, J. R.; Czuchajowski, L., Characterization of conductive polymeric nickel(II) tetrakis(3-methoxy-4-hydroxy-phenyl)porphyrin as an anodic material for electrocatalysis. *Journal of the Electrochemical Society* **1991,** *138* (7), 2008-15.

35. Vermillion, F. J., Jr.; Pearl, I. A., Anodic reactions of simple phenolic compounds. *Journal of the Electrochemical Society* **1964,** *111* (12), 1392-1400.

36. Samet, Y.; Abdelhedi, R.; Savall, A., A study of the electrochemical oxidation of guaiacol. *Physical & Chemical News* **2002,** *8* (1), 89-99.

37. Holthuis, J. J. M.; Van Oort, W. J.; Roemkens, F. M. G. M.; Renema, J.; Zuman, P., Electrochemistry of podophyllotoxin derivatives. Part I. Oxidation mechanism of etoposide (VP 16-213). *Journal of Electroanalytical Chemistry and Interfacial Electrochemistry* **1985,** *184* (2), 317-29.

38. Ciszewski, A.; Milczarek, G., Polyeugenol-modified platinum electrode for selective detection of dopamine in the presence of ascorbic acid. *Anal. Chem.* **1999,** *71* (5), 1055-1061.

39. Brown, M. D.; Schoenfisch, M. H., Nitric Oxide Permselectivity in Electropolymerized Films for Sensing Applications. *ACS Sensors* **2016,** *1* (12), 1453-1461.

40. MacTaylor, C. E.; Ewing, A. G., Characterization of the effects of varying the pH and monomer concentrations of poly(oxyphenylene) insulating films on carbon fiber electrodes. *Electroanalysis* **1997,** *9* (10), 755-758.

41. Boger, D. L.; Weinreb, S. M., *Organic Chemistry (N. Y.), Vol. 47: Hetero Diels-Alder Methodology in Organic Synthesis*. 1987; p 366 pp.

42. Ban, Y.; Iwasaki, T.; Ohmizu, H., Natural Products and Pharmaceuticals. In *Organic electrochemistry: an introduction and a guide*, Lund, H.; Baizer, M. M., Eds. Marcel Dekker, Inc.: New York, NY, 1991; pp 765-786.

43. Buechi, G.; Mak, C.-P., Biomimetic syntheses of the neolignans guianine, burchellin, 2-epi,3a-epiburchellin and futoenone. *Journal of the American Chemical Society* **1977,** *99* (24), 8073-5.

44. Ueda, C.; Tse, D. C.-S.; Kuwana, T., Stability of catechol modified carbon electrodes for electrocatalysis of dihydronicotinamide adenine dinucleotide and ascorbic acid. *Anal. Chem.* **1982,** *54* (5), 850-6.

45. Borgmann, S., Electrochemical quantification of reactive oxygen and nitrogen: challenges and opportunities. *Analytical and Bioanalytical Chemistry* **2009,** *394* (1), 95-105.

46. Ciszewski, A.; Milczarek, G., Preparation and general properties of chemically modified electrodes based on electrosynthesized thin polymeric films derived from eugenol. *Electroanalysis* **2001,** *13* (10), 860-867.

47. Ciszewski, A.; Milczarek, G., A new Nafion-free bipolymeric sensor for selective and sensitive detection of nitric oxide. *Electroanalysis* **1998,** *10* (11), 791-793.

48. Patel, B. A.; Arundell, M.; Parker, K. H.; Yeoman, M. S.; O'Hare, D., Detection of Nitric Oxide Release from Single Neurons in the Pond Snail, Lymnaea stagnalis. *Anal. Chem.* **2006,** *78* (22), 7643-7648.

49. Hirakawa, K.; Imato, T.; Yamasaki, S.; Ohura, H., Electrochemical responses of a polyeugenol and overoxidized polypyrrole composite film modified graphite electrode to dopamine and ascorbic acid. *Proceedings - Electrochemical Society* **2004,** *2004-08* (Chemical Sensors VI), 438-443.

50. Okumura, L. L.; Stradiotto, N. R.; Rees, N. V.; Compton, R. G., Modifying glassy carbon (GC) electrodes to confer selectivity for the voltammetric detection of L-cysteine in the presence of DL-homocysteine and glutathione. *Electroanalysis* **2008,** *20* (8), 916-918.

51. Paul, D. W.; Prajapati, I.; Reed, M. L., Electropolymerized eugenol: Evaluation as a protective film for oxygen sensing. *Sensors and Actuators, B: Chemical* **2013,** *183*, 129-135.

52. Artificial cerebrospinal fluid (ACSF). *Cold Spring Harbor Protocols* **2011,** *2011* (9), pdb.rec065730.

53. Amatore, C.; Saveant, J. M.; Tessier, D., Charge transfer at partially blocked surfaces. A model for the case of microscopic active and inactive sites. *Journal of Electroanalytical Chemistry and Interfacial Electrochemistry* **1983,** *147* (1-2), 39-51.

54. Daum, P. H.; Enke, C. G., Electrochemical kinetics of the ferri-ferrocyanide couple on platinum. *Anal. Chem.* **1969,** *41* (4), 653-6.

55. Wijnen, M. D.; Smit, W. M., Square-wave electrolysis. IV. Results and discussion. *Recueil des Travaux Chimiques des Pays-Bas et de la Belgique* **1960,** *79*, 289-312.

3. Long-term Drifts in Sensitivity Caused by Biofouling of an Amperometric Oxygen Sensor

This chapter is reformatted from an article published in *Electroanalysis* with permission from John Wiley & Sons, Inc. publisher. The original publication can be found as "M. M. Patrick, J. M. Grillot, Z. M. Derden, D. W. Paul, *Electroanalysis* **2017**, *29*, 998."

3.1 Abstract

Changes in oxygen sensitivity of an poly(o-phenylenediamine) (PoPD) coated gold electrode was determined by constructing calibration curves in vitro. Oxygen sensitivities recorded in the presence of biofoulants were significantly different from those recorded in buffer; however, PoPD demonstrated its effectiveness in providing some resistance to changes in oxygen sensitivity over time compared to a bare electrode. Three sets of PoPD-coated electrodes were calibrated in simple electrolyte of phosphate buffered saline; each set yielding an average oxygen sensitivity of 0.58±0.03 mA/ppm, 0.68±0.01 mA/ppm, and 0.48±0.01 mA/ppm (n=4), which shows the electrode to electrode variation in the PoPD-coating/ electrode. These sets were correspondingly exposed to bovine serum albumin, fibrinogen, rat brain homogenate. Exposure to these biofoulants resulted in decreases in sensitivity ranging from 26–35% after immediate exposure. Furthermore, long-term exposure to some biofoulants causes significant decreases in sensitivity over a time period of 14 days. We also estimated through in vitro exposure to rat brain homogenate the errors that might be associated with current methods of calibration. Sensitivities to oxygen determined by precalibration resulted in a 50% error from the sensitivity found in vitro; the error from postcalibration after rinsing resulted in 25% error.

3.2 Introduction

Oxygen is of critical importance in many biological processes. Clinically, decreased dissolved oxygen levels in the brain are connected to brain damage caused by ischemic strokes or trauma. In general, patients with higher levels of brain oxygen tend to survive, while patients with lower brain oxygen levels do not. It is therefore vital to monitor the oxygen concentration in the brain in order to care for brain trauma victims. An absolute threshold value of brain oxygen is a critical piece of information required by clinicians; below this value, clinical intervention would need to take place. However, there has been difficulty obtaining this threshold value, as the oxygen values vary significantly from patient to patient (from 8.5 to 20 mmHg). Indeed, when the absolute readings between laboratories are considered (average varied between 0.5 and 5.6 mmHg), it was concluded that only differences in the probes or human error could account for these differences.[1] It is believed that these oxygen variations are a result of a change in the probe's sensitivity occurring after implantation, and the procedures used with in vitro calibration. There is anecdotal evidence for this, but as of yet there has not been a comprehensive study to prove this phenomenon, at least for oxygen. Currently the only invasive oxygen probe approved for clinical use is based on the Clark-type oxygen electrode design.[2] The Clark-type electrochemical oxygen probe measures the diffusion-limited current for the reduction of dissolved oxygen, which is directly proportional to the concentration of dissolved oxygen. The most common Clark-type electrode is composed of a metal cathode (gold) and a reference electrode (Ag/ AgCl) behind a thin layer of electrolyte solution and covered with a protective semi-permeable membrane.[3] However, Clark-type electrodes used in clinical work are unsuitable for use in small animals such as rats, largely due to their size and poor spatial resolution for obtaining measurements in distinctive brain regions.[2]

Unlike the cathode type, the Clark-type oxygen sensor does not lend itself to mass production, or inclusion into sensor arrays; advances in in vivo sensing are most likely to be made in both of these areas. Because of these limitations, the work presented in this study utilized a cathode-type electrode with a polymer membrane coating. Membranes for the cathode type oxygen sensor include: polyethylene, polypropylene, cellulose acetate, Teflon, and polystrol.[4] Poly-o phenylenediamine (PoPD) has been studied for use in glucose oxidase sensors[5] and is thought to be suitable for long term use in vivo.[6] All membrane covered sensors suffer from biofouling, instability, and loss of calibration to some degree. The measurements are suspected to be off, but by how much? This work reports the quantitative changes in sensitivity of a cathode type oxygen sensor due to long term exposure to various suspected foulants.

The membrane-covering thwarts biofouling of the bare electrode, lengthening useful life of the sensor. As with all amperometric sensors, the sensitivity to the analyte diffusing through the membrane is set by the membrane's permeability. All implanted devices are subject to responses from the body, including wound healing, leukocytes, protein adsorption, and eventual encapsulation.[7-9] Adsorption of proteins to surfaces occurs rapidly;[10] typically followed by protein denaturation or conformational changes.[11-12] In addition, the immune response's effect on implanted sensors is an ongoing and oft-studied problem. The adsorption of biomolecules, biofouling, of the membrane alters the permeability of the membrane, and hence the calibration of the sensor.[13] Although biofouling has not been directly observed in vivo, the characterization of the biofouling mechanism has been under study for years.[14]

There are a few quantitative studies that highlight changes in sensor sensitivity caused by biofouling. Glutamate sensors constructed by m- and o-phenylenediamine entrapment of the enzyme showed decreases in sensitivity and selectivity after in vivo implantation in less than 4

hours.[15-16] Electrodes with Nafion/PoPD polymer films stored in biofoulant bovine serum albumin (BSA) protein and L-a-phosphatidylethanolamine lipid solutions for 24 hours exhibited a 38% decrease in sensitivity to nitric oxide; additional sensitivity changes were not observed after 72 hours.[17] Liu et al employed a BSA pretreatment as a method to minimize biofouling (blocking) of in vivo carbon fiber electrode dopamine sensors which exhibited similar results for pre- and postcalibration.[18] Klueh studied the biofouling of glucose sensors in vitro, outlining the effects blood components have on the sensitivity to glucose.[7, 19] A number of strategies have been investigated to attempt to minimize biofouling of electrochemical devices, but more research is needed to better understand this phenomenon.[20]

There have been many coating methods that attempt to minimize the effect of biofouling on the oxygen sensor response. This includes a nitric oxide generation that actively inhibits biofouling[21], as well as various polymer membranes that resist fouling.[22] One method to minimize the effects of biofouling on bare electrodes has been to apply a large oxidizing or reducing potential directly before an electrochemical measurement in order to detach any adsorbed and undesirable components from the surface of the electrode (organic, aliphatic compounds).[23-25] Alternatively, there was also a reported method that changed the morphology of a gold electrode itself in order to minimize the effects of biofouling.[26] A few reports note success using zwitterionic-modified sensors.[27-29] Coating zwitterionic poly(carboxybetaine) hydrogel onto a glucose sensor minimized blood-materials interactions and extended the life of the sensor.[30] Although there are some successes, biofouling of sensor membranes remains problematic. Some investigators have come to the conclusion that the development of a non-biofouling membrane can never be realized.[19] If this is the case then it would be useful to quantitatively measure sensitivity changes caused by biofouling.

Here we show changes in oxygen sensitivity and permeability through the PoPD membrane due to exposure to various biofoulants, including BSA, fibrinogen, and rat brain homogenate. We also note the stability of the PoPD-modified electrode over a 14 day period. Oxygen sensitivity of a bare gold electrode was compared to that of a PoPD-coated gold electrode. Finally, we present in vitro data that estimate the errors for in vivo measurements using the aforementioned recalibration methods.

3.3 Experimental

3.3.1 Reagents

NaCl, KCl, $MgCl_2$, $CaCl_2$, NaH_2PO_4, Na_2HCO_3, D-glucose, o-phenylenediamine (oPD) monomer, BSA, fibrinogen, and phosphate buffered saline (PBS) were obtained from Aldrich, Alfa Aesar, Amresco, EMD chemicals, Fisher Scientific, J.T. Baker, Sigma, or VWR and were used as received. Solutions of oPD monomer (5 mM) were prepared in 10 mM PBS. Brain tissue was obtained from male Sprague-Dawley rats used for other IACUC-approved experimental studies and were provided by Dr. Julie Stenken of the University of Arkansas. All animal protocols followed the guidelines set forth by the National Institutes of Health for the Care and Use of Laboratory Animals. Immediately after harvest, brain tissue was homogenized in a 50% wt solution of 10 mM PBS using a Biospecs Tissue Tearor; the resulting solution was divided into 1 mL aliquots. 1% (wt/wt) solutions of BSA, fibrinogen, and homogenized rat brain were prepared in HPLC grade water. Unless otherwise stated, experiments were carried out in PBS solution, pH 7.4 (140 mM NaCl, 10 mM phosphate buffer, 3 mM KCl). Biofouling studies with fibrinogen were carried out in artificial cerebrospinal fluid (aCSF) (119 mM NaCl, 2.5 mM KCl, 1.3 mM $MgCl_2$, 2.5 mM $CaCl_2$, 1 mM NaH_2PO_4, 26.2 mM Na_2HCO_3, and 10 mM D-glucose).

3.3.2 Working Electrode Preparation

The 2 mm gold disk working electrodes were obtained from CH Instruments. They were treated by mechanical polish via Buehler alumina polish of 5.0 mm, 1.0 mm, 0.3 mm, and finally 0.1 mm grits, and rinsed thoroughly with HPLC grade water. Polymerization solutions of 5 mM oPD monomer were prepared by dissolving in 10 mM PBS and sonicating for 10 minutes.[31-32] PoPD-coated gold electrodes were produced by potential cycling from 0.25 V to +1.3 V vs Ag/AgCl (in sat'd KCl) reference for 30 cycles.[33] Electrodes were rinsed with HPLC grade water post-polymerization to remove loosely bound monomer. Unless otherwise stated, a CH Instruments 1030 A potentiostat, Ag/AgCl (in sat'd KCl) reference electrode, and platinum flag counter electrode were used for all experiments.

The electrolyte solutions were purged of oxygen by bubbling nitrogen and then ambient oxygen was allowed to re-dissolve. The dissolved oxygen concentration was measured using a YSI Pro20 oxygen meter (Yellow Springs, OH). Cyclic voltammograms (CVs) of varying dissolved oxygen concentrations were obtained at PoPD-coated and bare Au electrodes by potential cycling from 0 V to 1.0 V vs Ag/AgCl in sat'd KCl reference. Calibration curves were constructed by plotting the current value at -0.6 V vs Ag/AgCl in sat'd KCl reference against the dissolved oxygen concentration. Sensor sensitivity to oxygen is taken as the slope of this line.

3.3.3. PoPD Film Stability

The stability of the PoPD polymer film was studied over time by potential cycling from 0.5 V to -0.2 V vs Ag/AgCl in sat'd KCl reference using 5 mM $K_3Fe(CN)_6$ as a probe molecule in 10 mM PBS. The $K_3Fe(CN)_6$ peak current at +0.2 V vs Ag/AgCl in sat'd KCl reference from the resulting CV was plotted versus time to show the stability and integrity of the PoPD coating.

3.3.4 Oxygen Sensitivity with Exposure to Biofoulants

PoPD-coated and bare electrodes were exposed to biofoulant solutions for varying duration and oxygen calibration curves constructed as described above. The resulting sensitivities from the calibration curves at various duration of biofoulant exposure were then plotted versus time, giving an indication of how the oxygen sensitivity changes over time with exposure to biofoulant.

3.4 Results and Discussion

Biofouling is well known to diminish the sensitivity of amperometric sensors. The hypothesis is that if a biofoulant adsorbs on a sensor surface, the rate of oxygen reduction will be impeded, and thus the oxygen sensitivity will decrease. The data presented in this study provides estimates about the magnitude of errors arising from in vivo oxygen sensors.

We chose to electropolymerize PoPD as this polymer was reportedly one of the most resistant to biofouling in vivo.[5-6] Electropolymerization offers the advantage of uniform and repeatable polymer coatings, and it also allows for selective coatings on individual members on an electrochemical array.[34]

3.4.1 PoPD Film Stability

The PoPD-coated electrodes were continuously exposed to 10 mM PBS for a period of two weeks. The long-term stability, e. g. cracking, or loss of adherence to the electrode, was determined by cyclic voltammetry of $[Fe(CN)_6]^{3-}$ (ferricyanide) at a bare and a PoPD-coated gold electrode; ferricyanide is an electrochemical probe molecule that gives a current response when in contact with an uncoated electrode surface. As Figure 3.1 shows, the bare electrode records larger but irregular ferricyanide current signals over time, while the PoPD-coated exhibits a relatively constant peak signal value at a significantly lower current value.

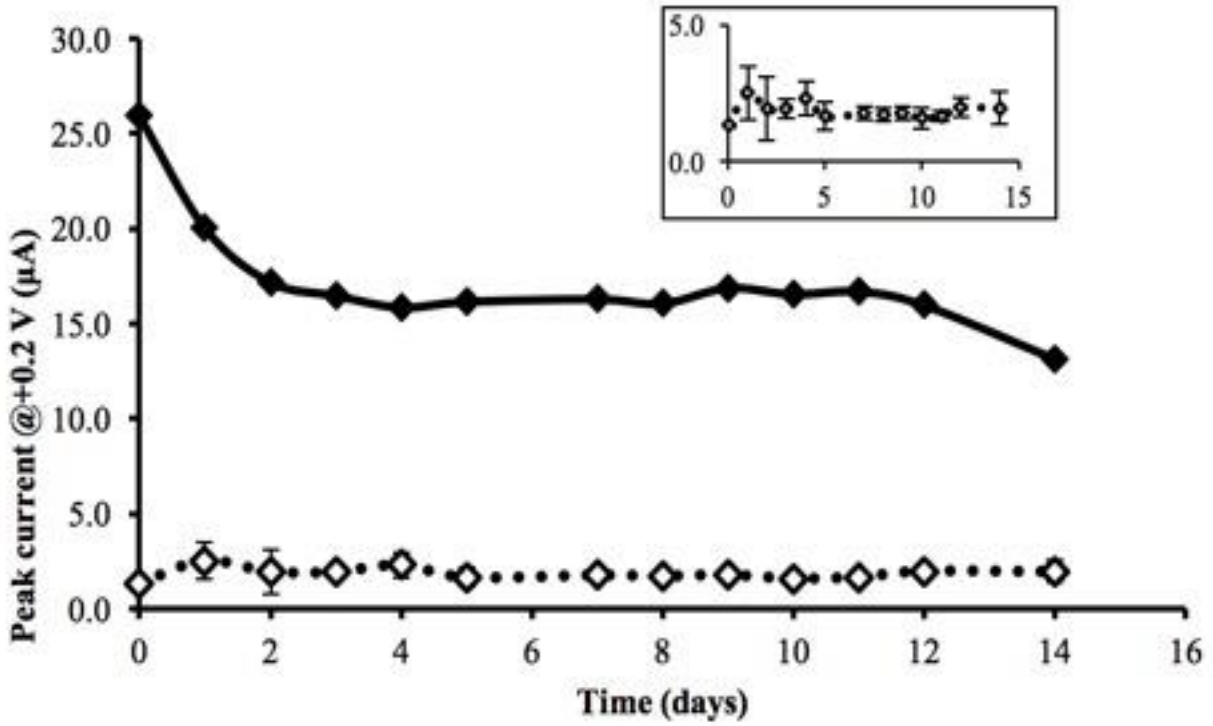

Figure 3.1 PoPD membrane stability in 10 mM PBS. PoPD-coated (n=3) and bare (n=1) electrodes are represented by open and solid diamonds, respectively. Inset is an expanded view which shows the day-to-day variations in the PoPD-coated electrode; reference electrode: Ag/AgCl in sat'd KCl.

This indicates that the PoPD coating is stable, as the probe molecule is unable to contact the electrode surface generating a current response. There are slight (~4%) day-to-day variations in the PoPD-coated electrode as shown by the inset in Figure 3.1; these variations will be discussed in a later section. Ferricyanide peak current (@+0.2 V) over time indicates a stable and uniform PoPD coating; bare electrode data indicates adsorption of undesirable molecules to the surface of the gold, altering the peak current over time.

Alternatively, the same probe molecule can be used to follow the passivation of an electrode from biofouling. Ferricyanide has been used in several reports to study the effect of biofoulants on the activity of an electrode. For example, Wallace et al. noted a decrease in peak current and increase in peak splitting for ferricyanide when the gold electrode was incubated in human serum albumin and immunoglobulin G.[35] After 10 minutes, the peak currents were "indistinguishable from the background charging current," implying that the adsorbed protein hindered ferricyanide redox capability.[35]

A representative oxygen CV is shown in Figure 3.2. The increased magnitude of current on the PoPD-coated CV is due to increased charging current. The lack of a steady-state oxygen current plateau is due to the continuous diffusion of oxygen through the membrane. Such CVs were used to construct calibration curves by plotting the reduction current at -0.6 V against the dissolved oxygen value.

PoPD-coated electrodes not only show periodically longer stability than bare electrodes, but also retain permeability to oxygen. Figure 3.3 shows an overlay of oxygen current values taken at -0.6 V on PoPD-coated electrodes at 2.00 ppm dissolved oxygen, showing the day-to-day variation of the sensor current.[36] After day 3, the variation in the current levels increases indicating changes in the PoPD membrane between the three replicate electrodes studied.

3.4.2 Oxygen Sensitivity Changes with Exposure to BSA

Serum albumin is a dominant blood protein. Serum albumin undergoes reversible adsorption depending on the type of surface it is in contact with.[37] The protein sequence and secondary structure of BSA were firstly proposed by Brown to be composed of three domains, over which there are nine sulfide loops.[38] At physiological pH, the three-dimensional structure is known to be a heart-shaped protein with an equilateral triangle of 80 Å and 30 Å deep. Compared to other proteins it is difficult to denature (80°C), and changes conformational structure with varying pH. Most interestingly these conformational changes are reversible. The protein presents itself as negatively charged, and the distribution of charge is evenly distributed over the surface.[39] Albumin is readily adsorbed on surfaces but can be displaced by other proteins.

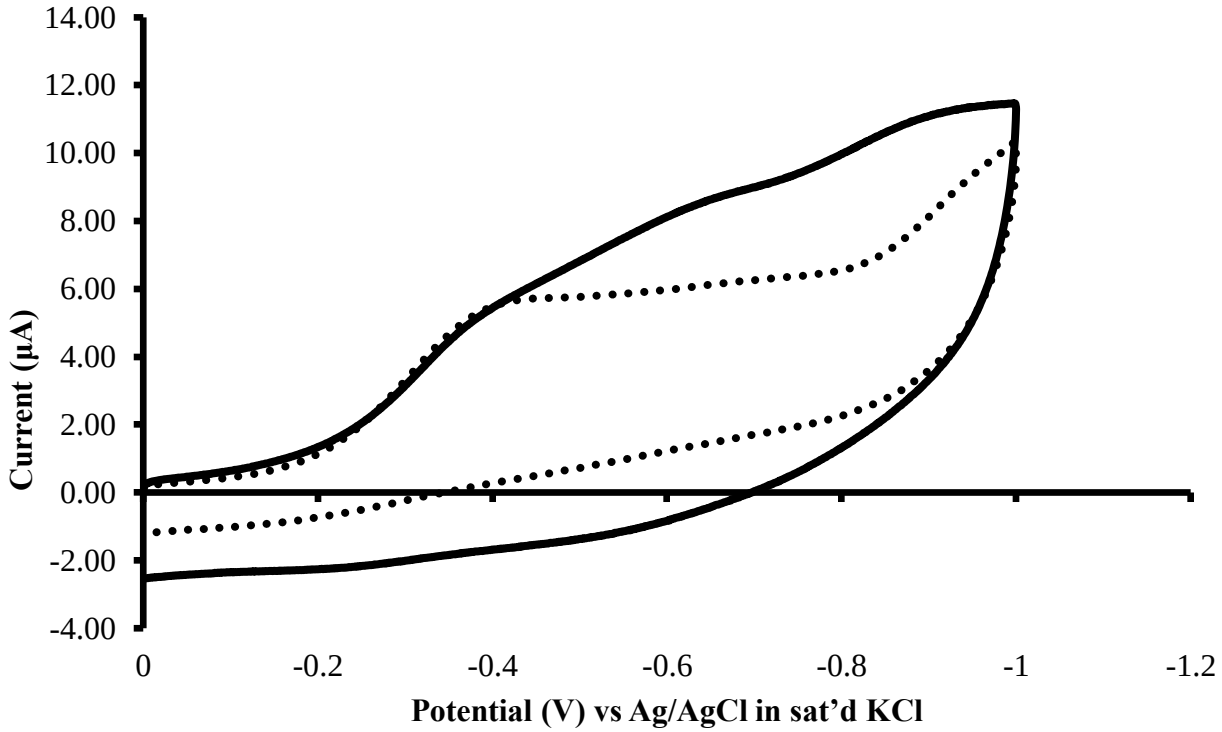

Figure 3.2 Representative cyclic voltammogram (CV) of ambient dissolved oxygen (6.50 ppm) in 10 mM PBS of PoPD-coated (solid line) and bare (dotted line) electrodes, which shows the typical reduction waves of oxygen at a gold electrode in neutral phosphate buffers; Ag/AgCl in sat'd KCl reference electrode.

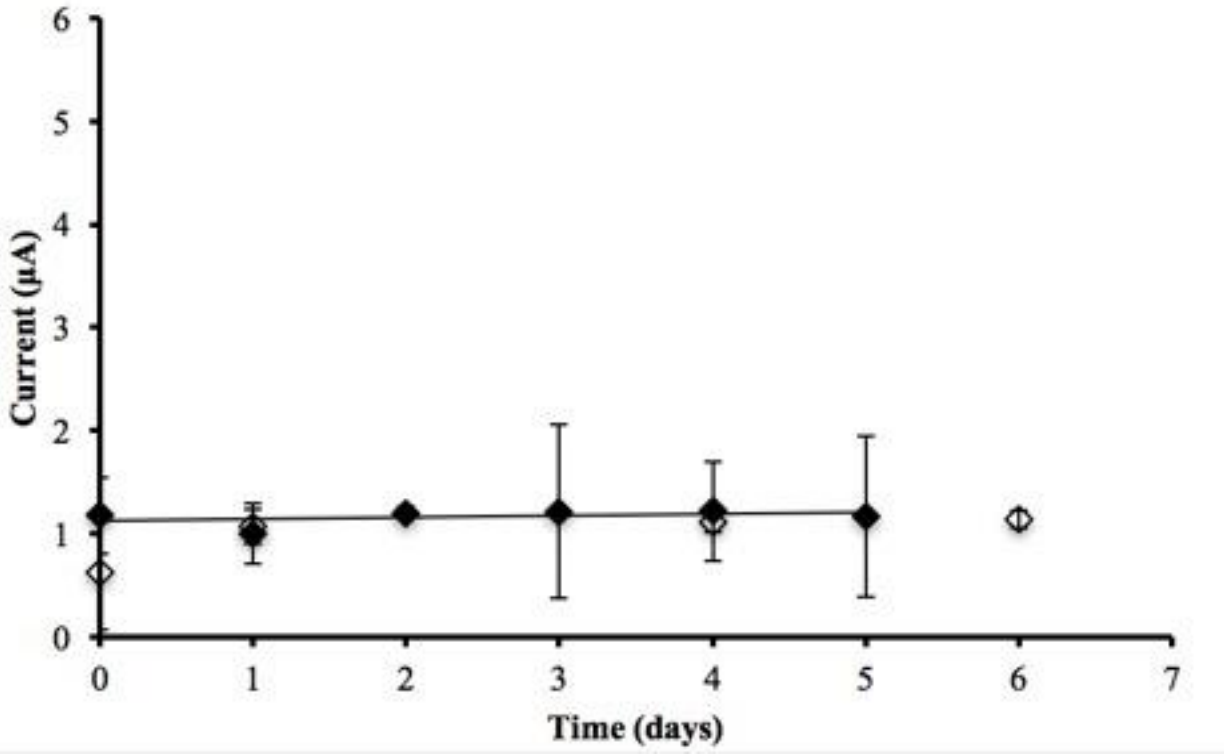

Figure 3.3 PoPD-coated electrode day-to-day variation. The current response at -0.6 V vs Ag/AgCl in sat'd KCl reference at 2.00 ppm dissolved O_2 in aCSF (n=3, closed diamonds) and with BSA added (n=3, open diamonds). The line serves only to aid the eye.

Figure 3.4 shows a representative oxygen calibration curve comparing PoPD-coated electrodes in control electrolyte and after immediate incubation in 1% BSA, where the shown error bars represent the electrode-to-electrode variation. The loss in sensitivity after BSA exposure (decreased slope of open diamonds as compared to closed diamonds) is assumed to be caused by BSA adsorbing to the PoPD film and impeding the diffusion of oxygen to the electrode.

Each point in Figure 3.5 represents the sensitivity of the oxygen sensor taken as the slope of the calibration curve (such as those shown in Figure 3.4); each data point represents the slope of the calibration curves (ordinate) obtained after the electrodes were incubated for a specific time (abscissa) in either aCSF or aCSF/BSA. Immediately upon exposure (<1 hour) to BSA in aCSF (Day 0 in Figure 3.5), the oxygen sensitivity for the PoPD-coated electrode shows a decrease in sensitivity of 46% (0.59±0.01 mA/ppm, and 0.32±0.01 mA/ppm). After 1 day of exposure to BSA in aCSF, the oxygen sensitivity increases to within 6% of the control values for PoPD-coated (0.50±0.03 mA/ppm control to 0.53±0.09 mA/ppm fouled).

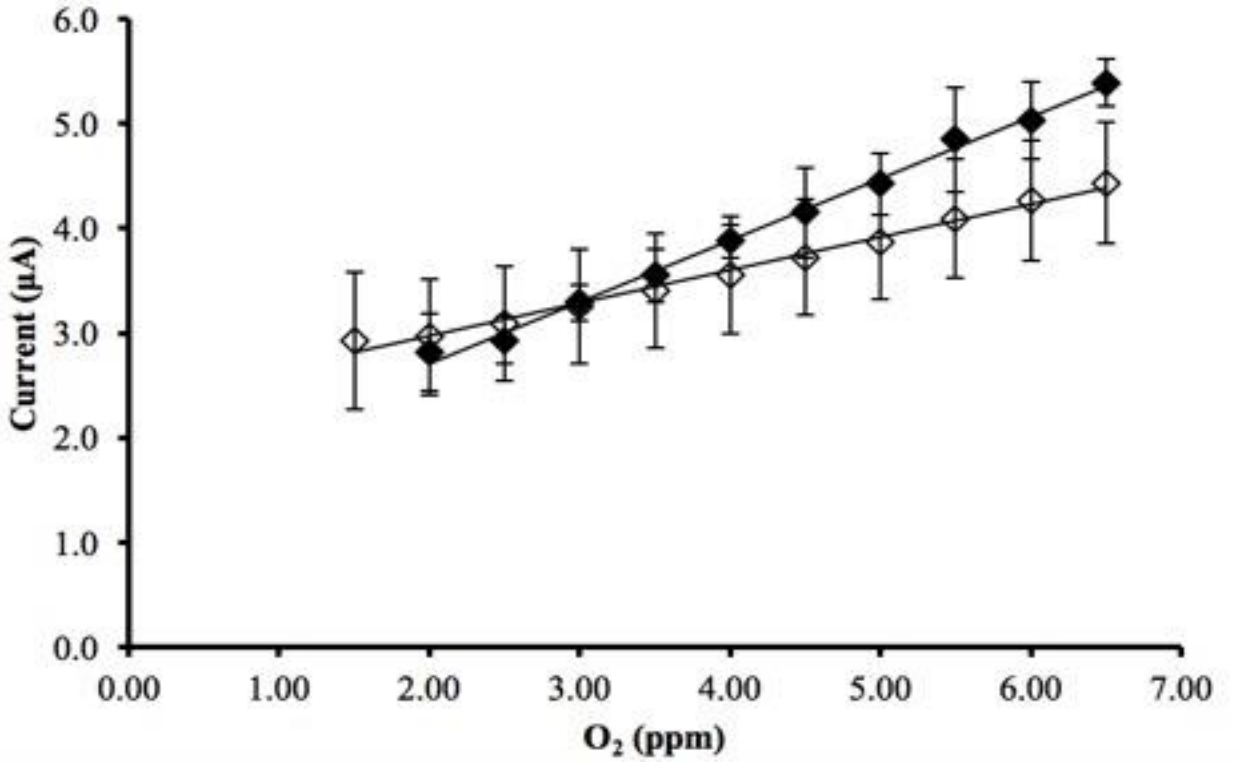

Figure 3.4 Representative oxygen calibration curve of PoPD-coated in control aCSF electrolyte (solid diamonds, n=3) and in test solution aCSF/BSA (open diamonds, n=3) in 10 mM PBS immediately after exposure to biofoulant, BSA (t=0 days). The sensitivities are taken as the slope of the resulting calibration curve; in aCSF: 0.590.01 mA/ppm O_2, in aCSF/BSA: 0.320.01 mA/ppm O_2; Ag/AgCl in sat'd KCl reference electrode.

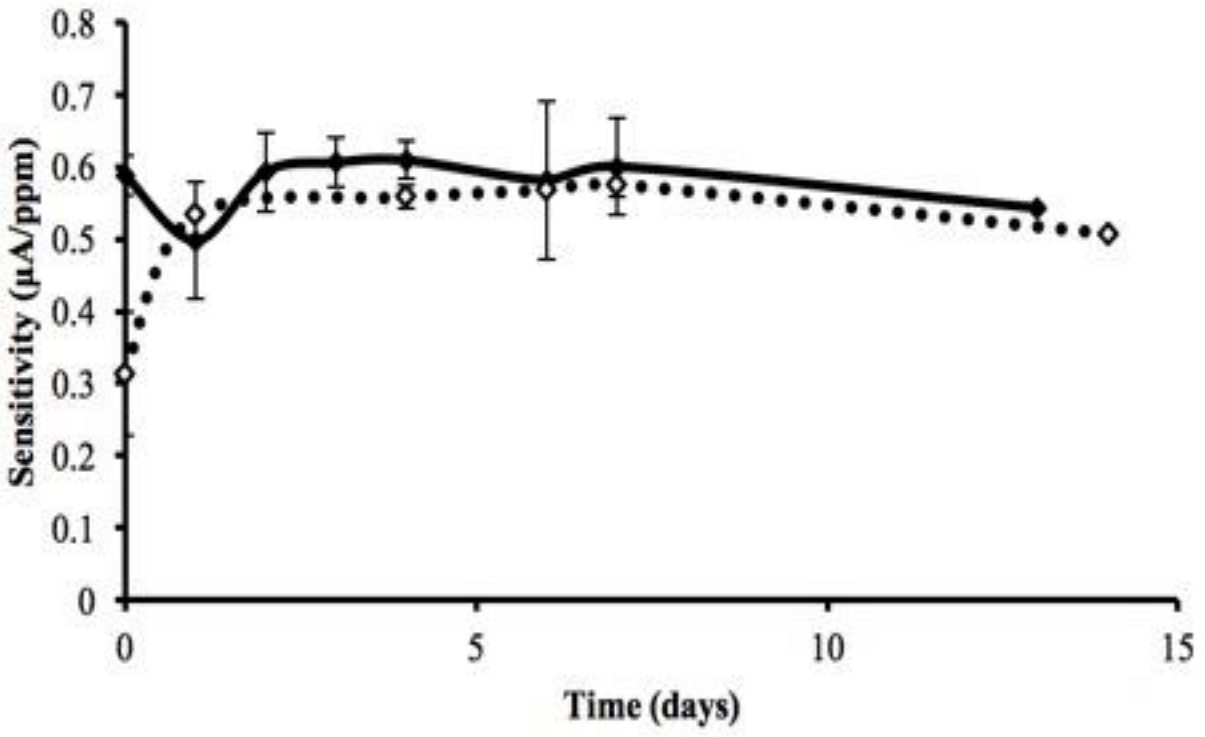

Figure 3.5 Oxygen sensitivity over time of PoPD-coated electrodes in control aCSF electrolyte (solid diamonds, n=3) and in test biofoulant aCSF/BSA solution (open diamonds, n=3).

The oxygen sensitivity of a bare gold electrode exposed to BSA follows the same trend as that for a PoPD-coated electrode. Immediately upon exposure to BSA the bare electrode (data not shown, n=1) shows a 51% decrease in sensitivity compared to the control (0.70 mA/ppm to 0.34 mA/ppm); after 1 day of exposure the bare electrode shows a 11% decrease in oxygen sensitivity (0.70 mA/ppm control to 0.62 mA/ppm fouled). This indicates that both the PoPD-coated and bare electrodes recover from fouling of BSA after 1 day. These results indicate that BSA is likely not the primary fouling component causing significant errors after time periods longer than 1 day. These results are in agreement with Bolger, et. al, who reported data after only 24 hours of BSA exposure on a PoPD-coated platinum microelectrode.[40] This is also consistent with the adsorption behavior of BSA mentioned above. The PoPD coating resists changes in oxygen sensitivity due to BSA fouling as compared to a bare electrode; however, PoPD does not eliminate the effects of fouling entirely.

3.4.3 Oxygen Sensitivity Changes with Exposure to Fibrinogen

Fibrinogen is a known biofoulant and is therefore frequently used in biofouling studies. Both BSA and fibrinogen are major components in blood plasma and are known to adsorb onto gold.[35, 41-43] BSA is a globular protein of approximately 66 kDa M.W.; fibrinogen is considerably larger at approximately 340 kDa.[44] Fibrinogen is a cell adhesive protein that is a major component in blood coagulation, and the third most prevalent protein in plasma with a concentration of 2.6-3.0 mg/mL.[45] Fibrinogen is a "sticky," high molecular weight protein that adsorbs to both hydrophilic and hydrophobic surfaces.[46] For its size it has a low charge density but shows separate regions of positive and negative charge. At pH 7.4, the uncompensated charge per fibrinogen molecule is 7.6 from the Lorenz-Stokes relationship, which could explain the substantial adsorption onto neutral and positively charged surfaces.[45] In addition, it has been

shown that near the isoelectric point (5.8), fibrinogen adsorbs in multilayers due to the strong lateral interactions and close packing, while at much higher and lower pH (>9 and <4), monolayers of fibrinogen are observed.[45-46] The experimental pH presented here (7.4) should lead to strong adsorption of fibrinogen to the polymer surface. Furthermore, it has been shown that fibrinogen exhibits strong and spontaneous adsorption onto gold substrates that are negatively polarized, which is the case in the work presented here.[47]

For brevity, the oxygen calibration curves for fibrinogen and rat brain homogenate biofouling studies have been omitted, and we only report the sensitivities found from the calibration curves. As shown in Figure 3.6, the PoPD-coated electrode (n=4) exhibited a decreased oxygen sensitivity when incubated in 1% fibrinogen solution. Immediately following fibrinogen exposure, the PoPD-coated electrode showed a 17% decrease in oxygen sensitivity (0.48±0.02 mA/ppm, as compared to the control electrolyte sensitivity of 0.58±0.02 mA/ppm); after prolonged exposure (19 days), the PoPD-coated showed only a 19% decrease (0.52±0.01 mA/ppm as compared to control electrolyte at 19 days 0.65±0.02 mA/ppm). The bare electrode (data not shown, n=1) showed a 26.9% decrease in oxygen sensitivity (from 0.67 mA/ppm to 0.49 mA/ppm); after 19 days of exposure the bare electrode showed a 52% decrease (from control value 0.91 mA/ppm to 0.44 mA/ppm after fibrinogen exposure). This suggests that PoPD protects the electrode surface from fibrinogen fouling, as the oxygen sensitivity at the bare electrode was essentially halved. The data points at 12 days are likely due to fluctuations of the control sensor from day-to-day. It is also of interest to note that, while the BSA study indicates that the sensor recovers near its original sensitivity, exposure to fibrinogen causes a permanent decrease in the sensitivity of the sensor.

3.4.4 Oxygen Sensitivity Changes with Exposure to Rat Brain Homogenate

One would expect rat brain homogenate to have the most extensive fouling properties, as it contains all brain matter, including proteins such as BSA and fibrinogen, as well as glial cells and lipids. Indeed, with exposure to rat brain homogenate, Figure 3.7 shows that the PoPD coated electrode exhibits a 43% decrease in oxygen sensitivity (0.37±0.02 mA/ppm initial incubation compared to the control PBS sensitivity value of 0.690.02 mA/ppm).

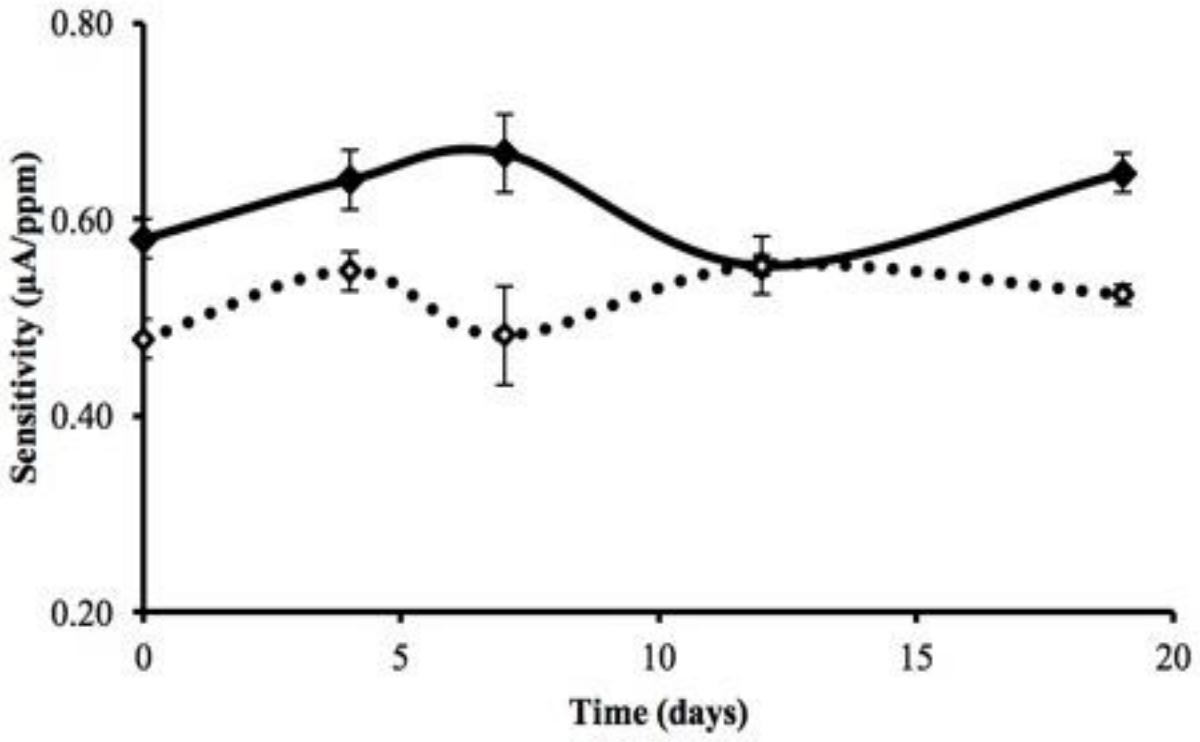

Figure 3.6 Oxygen sensitivity over time of PoPD-coated electrodes in control aCSF electrolyte (solid diamonds, n=4) and in test biofoulant aCSF/fibrinogen solution (open diamonds, n=4).

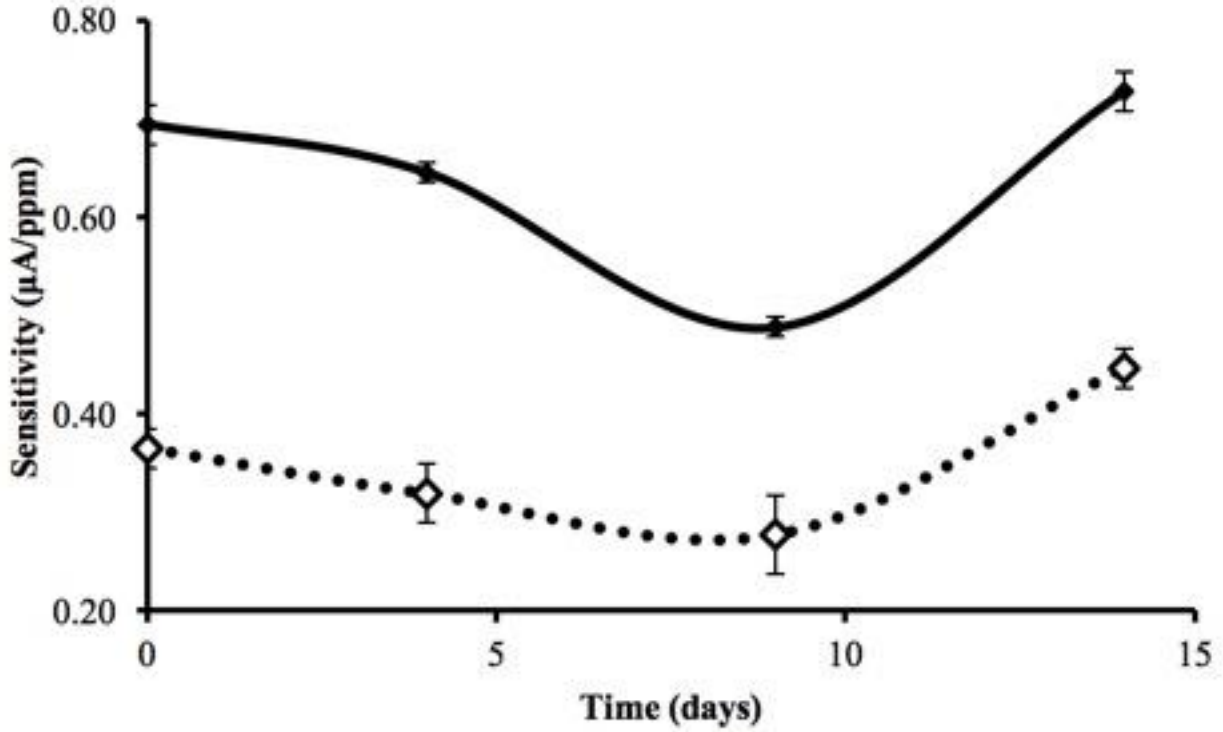

Figure 3.7 Oxygen sensitivity over time of PoPD-coated electrodes in control 10 mM PBS electrolyte (solid diamonds, n=4) and in test biofoulant 10 mM PBS/rat brain homogenate solution (open diamonds, n=4).

After 2 weeks of incubation, the PoPD-coated electrode exhibited a 38% decrease in sensitivity in biofouling solution (0.45±0.02 mA/ppm compared to the sensitivity obtained in control PBS 0.73±0.02 mA/ppm at 14 days). The bare electrode (data not shown, n=1) exhibits a 28% initial decrease in oxygen sensitivity (control value of 0.79 mA/ppm to 0.57 mA/ppm after initial exposure); with exposure over 2 weeks the oxygen sensitivity for the bare electrode shows a 26% decrease in oxygen sensitivity compared to the control PBS value at 14 days (0.74 mA/ ppm to 0.55 mA/ppm). Sensitivity changes for the PoPD-coated electrode in the presence of rat brain homogenate follows the same trend as that for the control electrolyte. This could indicate that the rat brain homogenate causes a fixed and permanent change to the PoPD layer, but the PoPD membrane itself changes with time (Fig. 3.2). Such variations in the PoPD layer are difficult to justify or quantify. In general, variations in sensitivity of the bare electrode (data not shown) are more extreme than those of the PoPD-coated.

The oxygen sensitivity of the PoPD-coated sensor varies over time while being incubated in an electrolyte (Figs. 3.5, 3.6, 3.7). This indicates that there could be changes in PoPD permeability to oxygen over time. These variations are greater than the uncertainty in the experimental determinations of sensitivity. The inset of Fig. 3.1 indicates that the PoPD layer is dynamic, changing over time. The cause of this variability is not known, but these types of studies have not been done before.

3.4.5 Simulation of in vivo Recalibration Practices

For sensors calibrated in vitro then implanted, the matrix of the calibration solution should reflect that of the in vivo matrix. Keddie and Rohman noted that differences between the calibration solution and in vivo test environment most assuredly cause the probe to function "differently."[48] The main differences between in vivo and in vitro calibrations are: the mass

transport through a standard solution is different due to diffusion and convection, and there are numerous interferences from a complex sample matrix in vivo causing the limited operational stability of sensors in biological media.[49-52] In addition, Kealy et. al expressed the need for caution when using in vitro calibrations to estimate in vivo concentrations because of key differences between in vitro solution and the in vivo matrix, namely "capacitance, current, diffusion, sensitivity, etc…."[53] It is therefore unreasonable to calibrate the sensor in electrolyte and expect the sensitivity to be the same in vivo. Indeed, McHugh, et al., noted that "electrode responses in vivo may not be the same ex vivo,"[54] and Singh, et al., stated that "postcalibration alone or averaging of pre- and postcalibration is likely to lead to over- or underestimation of analyte concentrations."[55] Despite this information, a number of researchers continue to utilize the practice of applying in vitro calibrations toward interpreting in vivo measurements.[52-53, 56-57] For current in vivo recalibration practices for various sensors the electrode is calibrated in electrolyte solution to obtain the sensitivity value, implanted, and then recalibrated upon removal of the probe, again in electrolyte.[54-55, 58-60] If the sensitivity changes pre- and postcalibration then the sensitivity from the post-implantation is taken. Meyerhoff made the assertion that analyte values measured by the implanted blood-gas sensors decrease from corresponding in vitro measurements, but when removed and retested in vitro, "very accurate results are often obtained."[61]

We mimicked this process in vitro by calibrating the probe in an electrolyte solution, immediately after biofoulant exposure (t=0), 24 hours after biofoulant exposure, and again in the same, but fresh, electrolyte solution after a thorough rinsing. As is evident in Fig. 3.8(A), the oxygen sensitivity decreases significantly for both PoPD-coated and bare electrodes when exposed to BSA for 24 hours, followed by an increase when rinsed and recalibrated in

electrolyte. The PoPD-coated electrode returns to the original sensitivity within experimental error, whereas the bare electrode remains at a decreased value. The decreases in sensitivity range from 26–35% after immediate exposure to the biofoulants. Similar trends can be seen in Fig. 3.8(B) with fibrinogen exposure, except that the sensitivity remains decreased even after rinsing.

It is well known that sensor sensitivity drifts in vivo, but the in vitro data presented in Fig. 3.8(C) simulates what the drift in sensitivity might be. A major question is the magnitude of the error. By only considering the results obtained in the presence of the rat brain homogenate, the current procedure of using in vitro oxygen calibration pre- or post-implantation may report oxygen values that are off by as much as 30% (black or striped compared to gray or white). If rat brain homogenate is assumed to be similar to in vivo conditions, then the in vivo oxygen readings are in error by as much as 50% (black/striped to grey). The in vitro results suggest that oxygen values are most likely higher than what is actually reported by the sensor using pre- or post-calibrations.

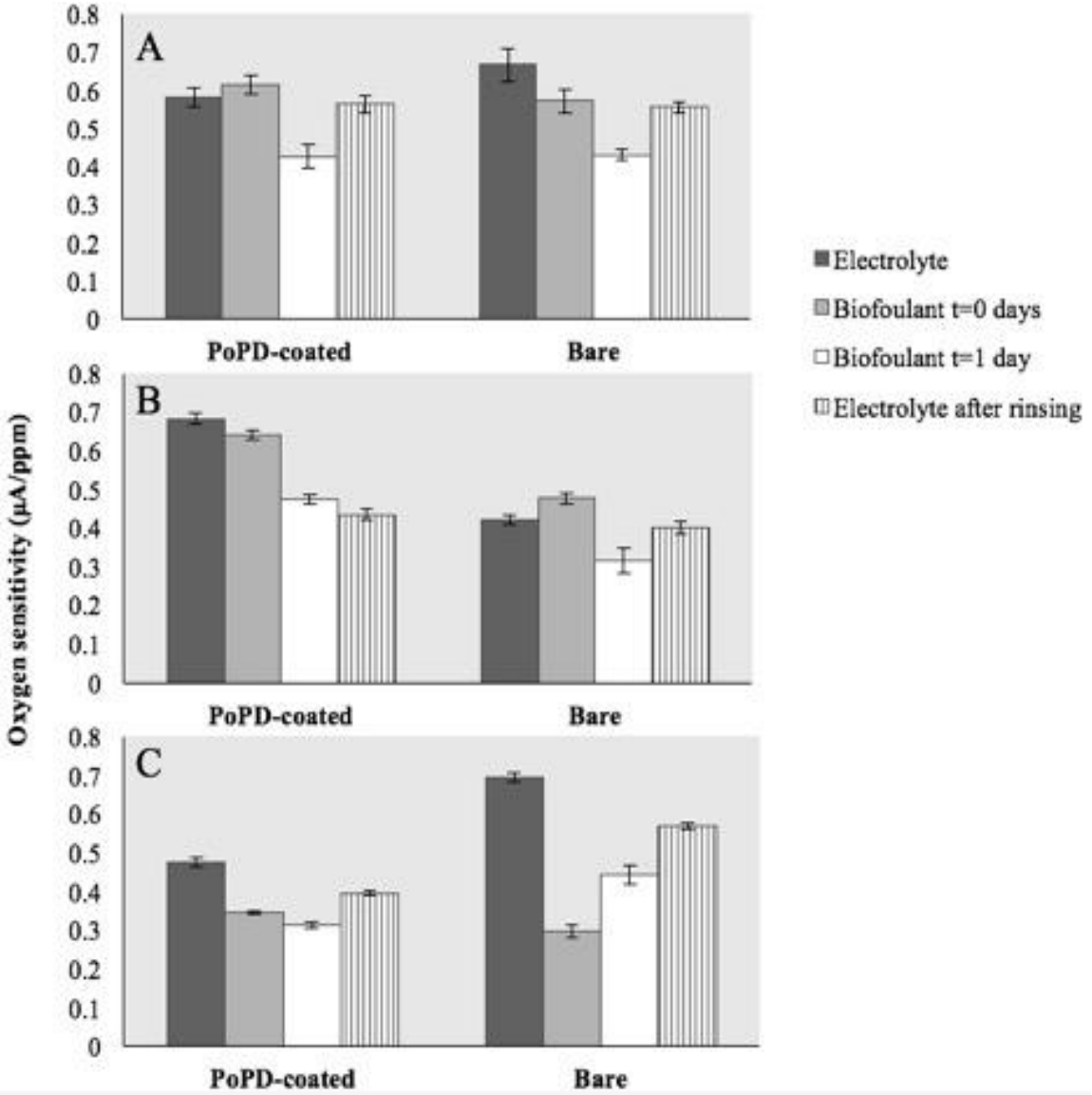

Figure 3.8 Oxygen sensitivities from a mimic of in vivo recalibration methods with exposure to: A. BSA, B. Fibrinogen, and C. Rat brain homogenate.

3.5 Conclusion

This study is the first to quantify the changes in sensitivity for oxygen sensors upon long-term exposure to biofoulants using PoPD-coated gold electrodes. Data from in vivo sensors are affected by protein adsorption to the membrane, and therefore changes in sensitivity of the probe over time; potentially causing errors in the oxygen measurements. Different biofouling behavior was discussed as a proof of concept here. However, as most implantable oxygen sensors are Clark type microelectrodes with a larger surface to volume ratio, the kinetics and fouling are different from disk electrode discussed here. Therefore, the conclusion may not be directly transferable to in vivo sensors. In the Introduction section we referred to a study of brain oxygen levels that were not in agreement with each other;[62-63] moreover, adjacent implanted sensors reported significantly different sensor responses. Sensitivity changes appear unique to each sensor, and also to each implantation. Since a membrane that resists all biofouling is currently unavailable, the solution to drifting sensitivity is to consider an in vivo calibration scheme after implantation.

3.6 Acknowledgements

The authors acknowledge financial support from the Arkansas Biosciences Institute, the major research component of the Arkansas Tobacco Settlement Proceeds Act of 2000. We are also thankful for the collaborative support of Dr. Julie Stenken's research group, especially Tina Poseno.

3.7 References

1. Nozue, M.; Lee, I.; Yuan, F.; Teicher, B. A.; Brizel, D. M.; Dewhirst, M. W.; Milross, C. G.; Milas, L.; Song, C. W.; Thomas, C. D.; Guichard, M.; Evans, S. M.; Koch, C. J.; Lord, E. M.; Jain, R. K.; Suit, H. D., Interlaboratory variation in oxygen tension measurement by Eppendorf "Histograph" and comparison with hypoxic marker. *Journal of surgical oncology* **1997,** *66* (1), 30-8.

2. Dengler, J.; Frenzel, C.; Vajkoczy, P.; Wolf, S.; Horn, P., Cerebral tissue oxygenation measured by two different probes: challenges and interpretation. *Intensive Care Medicine* **2011,** *37* (11), 1809-1815.

3. Clark, L. C., Jr.; Wold, R.; Granger, D.; Taylor, Z., Continuous recording of blood oxygen tensions by polarography. *Journal of Applied Physiology (1948-1976)* **1953,** *6*, 189-93.

4. Severinghaus, J. W.; Astrup, P. B., History of blood gas analysis. V. Oxygen measurement. *Journal of clinical monitoring* **1986,** *2* (3), 174-89.

5. Rothwell, S. A.; Killoran, S. J.; O'Neill, R. D., Enzyme immobilization strategies and electropolymerization conditions to control sensitivity and selectivity parameters of a polymer-enzyme composite glucose biosensor. *Sensors* **2010,** *10*, 6439-6462.

6. Killoran, S. J.; O'Neill, R. D., Characterization of permselective coatings electrosynthesized on Pt-Ir from the three phenylenediamine isomers for biosensor applications. *Electrochimica Acta* **2008,** *53* (24), 7303-7312.

7. Klueh, U.; Liu, Z.; Ouyang, T.; Cho, B.; Feldman, B.; Henning Timothy, P.; Kreutzer, D., Blood-induced interference of glucose sensor function in vitro: implications for in vivo sensor function. *Journal of diabetes science and technology* **2007,** *1* (6), 842-9.

8. Ratner, B. D.; Bryant, S. J., Biomaterials: Where we have been and where we are going. *Annual Review of Biomedical Engineering* **2004,** *6*, 41-75.

9. Anderson, J. M.; Rodriguez, A.; Chang, D. T., Foreign body reaction to biomaterials. *Seminars in Immunology* **2008,** *20* (2), 86-100.

10. Higson, S. P. J.; Desai, M. A.; Ghosh, S.; Christie, I.; Vadgama, P., Amperometric enzyme electrode biofouling and passivation in blood: Characterization of working electrode

polarization and inner membrane effects. *Journal of the Chemical Society, Faraday Transactions* **1993,** *89* (15), 2847-51.

11. Collyer, S.; Davis, F.; Lucke, A.; Stirling, C. J. M.; Higson, S. P. J., An investigation into outer-surface biofouling and electrode passivation effects on gold electrodes modified with calix[4]resorcinarenetetrathiol and a PEG derivative on exposure to whole human blood. *Electroanalysis* **2004,** *16* (4), 275-281.

12. Sadana, A., Protein adsorption and inactivation on surfaces. Influence of heterogeneities. *Chemical Reviews (Washington, DC, United States)* **1992,** *92* (8), 1799-818.

13. Barfidokht, A.; Gooding, J. J., Approaches Toward Allowing Electroanalytical Devices to be Used in Biological Fluids. *Electroanalysis* **2014,** *26* (6), 1182-1196.

14. Andrade, J. D., Interfacial phenomena and biomaterials. *Medical Instrumentation* **1973,** *7* (2), 110-20.

15. Wisniewski, N.; Moussy, F.; Reichert, W. M., Characterization of implantable biosensor membrane biofouling. *Fresenius' Journal of Analytical Chemistry* **2000,** *366* (6-7), 611-621.

16. Wahono, N.; Qin, S.; Oomen, P.; Cremers, T. I. F.; de Vries, M. G.; Westerink, B. H. C., Evaluation of permselective membranes for optimization of intracerebral amperometric glutamate biosensors. *Biosens. Bioelectron.* **2012,** *33* (1), 260-266.

17. Brown, F. O.; Finnerty, N. J.; Lowry, J. P., Nitric oxide monitoring in brain extracellular fluid: characterisation of Nafion-modified Pt electrodes in vitro and in vivo. *Analyst (Cambridge, U. K.)* **2009,** *134* (10), 2012-2020.

18. Liu, X.; Zhang, M.; Xiao, T.; Hao, J.; Li, R.; Mao, L., Protein Pretreatment of Microelectrodes Enables in Vivo Electrochemical Measurements with Easy Precalibration and Interference-Free from Proteins. *Analytical Chemistry (Washington, DC, United States)* **2016,** *88* (14), 7238-7244.

19. Klueh, U., Analysis: on the path to overcoming glucose-sensor-induced foreign body reactions. *Journal of diabetes science and technology* **2013,** *7* (2), 452-4.

20. Hanssen, B. L.; Siraj, S.; Wong, D. K. Y., Recent strategies to minimise fouling in electrochemical detection systems. *Reviews in Analytical Chemistry* **2016,** *35* (1), 1-28.

21. Ren, H.; Coughlin, M. A.; Major, T. C.; Aiello, S.; Rojas Pena, A.; Bartlett, R. H.; Meyerhoff, M. E., Improved in Vivo Performance of Amperometric Oxygen (PO2) Sensing Catheters via Electrochemical Nitric Oxide Generation/Release. *Analytical Chemistry (Washington, DC, United States)* **2015,** *87* (16), 8067-8072.

22. Vreeland, R. F.; Atcherley, C. W.; Russell, W. S.; Xie, J. Y.; Lu, D.; Laude, N. D.; Porreca, F.; Heien, M. L., Biocompatible PEDOT:Nafion Composite Electrode Coatings for Selective Detection of Neurotransmitters in Vivo. *Analytical Chemistry (Washington, DC, United States)* **2015,** *87* (5), 2600-2607.

23. Austin-Harrison, D. S.; Johnson, D. C., Pulsed amperometric detection based on direct and indirect anodic reactions: a review. *Electroanalysis (N. Y.)* **1989,** *1* (3), 189-97.

24. Johnson, D. C.; Dobberpuhl, D.; Roberts, R.; Vandeberg, P., Pulsed amperometric detection of carbohydrates, amines and sulfur species in ion chromatography. The current state of research. *Journal of Chromatography* **1993,** *640* (1-2), 79-96.

25. Khubutiya, M. S.; Evseev, A. K.; Kolesnikov, V. A.; Goldin, M. M.; Davydov, A. D.; Volkov, A. G.; Stepanov, A. A., Measurements of platinum electrode potential in blood and blood plasma and serum. *Russian Journal of Electrochemistry* **2010,** *46* (5), 537-541.

26. Patel, J.; Radhakrishnan, L.; Zhao, B.; Uppalapati, B.; Daniels, R. C.; Ward, K. R.; Collinson, M. M., Electrochemical Properties of Nanostructured Porous Gold Electrodes in Biofouling Solutions. *Analytical Chemistry (Washington, DC, United States)* **2013,** *85* (23), 11610-11618.

27. Gui, A. L.; Luais, E.; Peterson, J. R.; Gooding, J. J., Zwitterionic Phenyl Layers: Finally, Stable, Anti-Biofouling Coatings that Do Not Passivate Electrodes. *ACS Applied Materials & Interfaces* **2013,** *5* (11), 4827-4835.

28. Ladd, J.; Zhang, Z.; Chen, S.; Hower, J. C.; Jiang, S., Zwitterionic Polymers Exhibiting High Resistance to Nonspecific Protein Adsorption from Human Serum and Plasma. *Biomacromolecules* **2008,** *9* (5), 1357-1361.

29. Cheng, G.; Li, G.; Xue, H.; Chen, S.; Bryers, J. D.; Jiang, S., Zwitterionic carboxybetaine polymer surfaces and their resistance to long-term biofilm formation. *Biomaterials* **2009,** *30* (28), 5234-5240.

30. Yang, W.; Xue, H.; Carr, L. R.; Wang, J.; Jiang, S., Zwitterionic poly(carboxybetaine) hydrogels for glucose biosensors in complex media. *Biosens. Bioelectron.* **2011,** *26* (5), 2454-2459.

31. Dai, Y.-Q.; Zhou, D.-M.; Shiu, K.-K., Permeability and permselectivity of polyphenylenediamine films synthesized at a palladium disk electrode. *Electrochimica Acta* **2006,** *52* (1), 297-303.

32. Kong, L.; Jiang, X.; Zeng, Y.; Zhou, T.; Shi, G., Molecularly imprinted sensor based on electropolmerized poly(o-phenylenediamine) membranes at reduced graphene oxide modified electrode for imidacloprid determination. *Sensors and Actuators, B: Chemical* **2013,** *185*, 424-431.

33. Zhai, W.; Tian, X.; Yan, Y.; Xu, Y.; Zhao, Y.; Liu, Y., Preparation and characterization of a poly-o-phenylenediamine film modified glassy carbon electrode as a H2O2 sensor. *Canadian Journal of Chemistry* **2013,** *91* (11), 1077-1084.

34. Gerard, M.; Chaubey, A.; Malhotra, B. D., Application of conducting polymers to biosensors. *Biosens. Bioelectron.* **2002,** *17* (5), 345-359.

35. Moulton, S. E.; Barisci, J. N.; Bath, A.; Stella, R.; Wallace, G. G., Investigation of protein adsorption and electrochemical behavior at a gold electrode. *Journal of Colloid and Interface Science* **2003,** *261* (2), 312-319.

36. Hoelper, B. M.; Alessandri, B.; Heimann, A.; Behr, R.; Kempski, O., Brain oxygen monitoring: in-vitro accuracy, long-term drift and response-time of Licox- and Neurotrend sensors. *Acta neurochirurgica* **2005,** *147* (7), 767-74; discussion 774.

37. Carter, D. C.; Ho, J. X., Structure of serum albumin. *Advances in Protein Chemistry* **1994,** *45* (LIPOPROTEINS,APOLIPOPROTEINS, AND LIPASES), 153-203.

38. Brown, J. R., Serum albumin: amino acid sequence. In *Albumin Structure, Function, and Uses*, Rosenoer, V. M.; Oratz, M.; Rotschild, M. A., Eds. Pergamon Press: Oxford, 1977; pp 27-51.

39. Peters, J., Theodore, Serum Albumin. *Advances in Protein Chemistry* **1985,** *37*, 161-245.

40. Bolger, F. B.; Bennett, R.; Lowry, J. P., An in vitro characterisation comparing carbon paste and Pt microelectrodes for real-time detection of brain tissue oxygen. *Analyst (Cambridge, U. K.)* **2011,** *136* (19), 4028-4035.

41. Moulton, S. E.; Barisci, J. N.; Bath, A.; Stella, R.; Wallace, G. G., Studies of double layer capacitance and electron transfer at a gold electrode exposed to protein solutions. *Electrochimica Acta* **2004,** *49* (24), 4223-4230.

42. Ying, P.; Viana, A. S.; Abrantes, L. M.; Jin, G., Adsorption of human serum albumin onto gold: a combined electrochemical and ellipsometric study. *Journal of Colloid and Interface Science* **2004,** *279* (1), 95-99.

43. Szott, L. M.; Horbett, T. A., Mechanisms of the foreign body response to RFGD plasma-generated PEO-like films. *ACS Symposium Series* **2012,** *1120* (Proteins at Interfaces III), 321-337.

44. Glomm, W. R.; Halskau, O., Jr.; Hanneseth, A.-M. D.; Volden, S., Adsorption Behavior of Acidic and Basic Proteins onto Citrate-Coated Au Surfaces Correlated to Their Native Fold, Stability, and pI. *Journal of Physical Chemistry B* **2007,** *111* (51), 14329-14345.

45. Wasilewska, M.; Adamczyk, Z.; Jachimska, B., Structure of Fibrinogen in Electrolyte Solutions Derived from Dynamic Light Scattering (DLS) and Viscosity Measurements. *Langmuir* **2009,** *25* (6), 3698-3704.

46. Feng, L.; Andrade, J. D., Structure and adsorption properties of fibrinogen. *ACS Symposium Series* **1995,** *602* (Proteins at Interfaces 2), 66-79.

47. Dargahi, M.; Konkov, E.; Omanovic, S., Influence of Surface Charge/Potential of a Gold Electrode on the Adsorptive/Desorptive Behaviour of Fibrinogen. *Electrochimica Acta* **2015,** *174*, 1009-1016.

48. Keddie, S.; Rohman, L., Reviewing the reliability, effectiveness and applications of Licox in traumatic brain injury. *Nursing in critical care* **2012,** *17* (4), 204-12.

49. Bucur, B., Technological barriers in the use of electrochemical microsensors and microbiosensors for in vivo analysis of neurological relevant substances. *Current Neuropharmacology* **2012,** *10* (3), 197-211.

50. Oleinick, A. I.; Amatore, C.; Guille, M.; Arbault, S.; Klymenko Oleksiy, V.; Svir, I., Modelling release of nitric oxide in a slice of rat's brain: describing stimulated functional hyperemia with diffusion-reaction equations. *Mathematical medicine and biology : a journal of the IMA* **2006,** *23* (1), 27-44.

51. Burmeister, J. J.; Gerhardt, G. A., Ceramic-based multisite microelectrode arrays for in vivo electrochemical recordings of glutamate and other neurochemicals. *TrAC, Trends Anal. Chem.* **2003,** *22* (8), 498-502.

52. Hu, Y.; Wilson, G. S., Rapid changes in local extracellular rat brain glucose observed with an in vivo glucose sensor. *J. Neurochem.* **1997,** *68* (4), 1745-1752.

53. Kealy, J.; Bennett, R.; Lowry John, P., Simultaneous recording of hippocampal oxygen and glucose in real time using constant potential amperometry in the freely-moving rat. *Journal of neuroscience methods* **2013,** *215* (1), 110-20.

54. McHugh, S. B.; Fillenz, M.; Lowry, J. P.; Rawlins, J. N. P.; Bannerman, D. M., Brain tissue oxygen amperometry in behaving rats demonstrates functional dissociation of dorsal and ventral hippocampus during spatial processing and anxiety. *The European journal of neuroscience* **2011,** *33* (2), 322-37.

55. Singh, Y. S.; Sawarynski, L. E.; Dabiri, P. D.; Choi, W.-W. R.; Andrews, A. M., Head-to-Head Comparisons of Carbon Fiber Microelectrode Coatings for Sensitive and Selective Neurotransmitter Detection by Voltammetry. *Analytical Chemistry (Washington, DC, United States)* **2011,** *83* (17), 6658-6666.

56. Xiang, L.; Yu, P.; Zhang, M.; Hao, J.; Wang, Y.; Zhu, L.; Dai, L.; Mao, L., Platinized Aligned Carbon Nanotube-Sheathed Carbon Fiber Microelectrodes for In Vivo Amperometric Monitoring of Oxygen. *Analytical Chemistry (Washington, DC, United States)* **2014,** *86* (10), 5017-5023.

57. Kuhr, W. G.; Ewing, A. G.; Caudill, W. L.; Wightman, R. M., Monitoring the stimulated release of dopamine with in vivo voltammetry. I: Characterization of the response observed in the caudate nucleus of the rat. *J. Neurochem.* **1984,** *43* (2), 560-9.

58. Logman, M. J.; Budygin, E. A.; Gainetdinov, R. R.; Wightman, R. M., Quantitation of in vivo measurements with carbon fiber microelectrodes. *J. Neurosci. Methods* **2000,** *95* (2), 95-102.

59. Bazzu, G.; Puggioni, G. G. M.; Dedola, S.; Calia, G.; Rocchitta, G.; Migheli, R.; Desole, M. S.; Lowry, J. P.; O'Neill, R. D.; Serra, P. A., Real-Time Monitoring of Brain Tissue Oxygen Using a Miniaturized Biotelemetric Device Implanted in Freely Moving Rats. *Analytical Chemistry (Washington, DC, United States)* **2009,** *81* (6), 2235-2241.

60. Gifford, R.; Kehoe, J. J.; Barnes, S. L.; Kornilayev, B. A.; Alterman, M. A.; Wilson, G. S., Protein interactions with subcutaneously implanted biosensors. *Biomaterials* **2006,** *27* (12), 2587-2598.

61. Meyerhoff, M. E., In vivo blood-gas and electrolyte sensors: progress and challenges. *TrAC, Trends in Analytical Chemistry* **1993,** *12* (6), 257-65.

62. Valadka, A. B.; Gopinath, S. P.; Contant, C. F.; Uzura, M.; Robertson, C. S., Relationship of brain tissue PO2 to outcome after severe head injury. *Critical care medicine* **1998,** *26* (9), 1576-81.

63. Sarrafzadeh, A. S.; Kiening, K. L.; Callsen, T. A.; Unterberg, A. W., Metabolic changes during impending and manifest cerebral hypoxia in traumatic brain injury. *British journal of neurosurgery* **2003,** *17* (4), 340-6.

4. Evaluation of PoPD on microelectrodes for oxygen sensitivity response in the presence of biofoulants and in situ calibration of biofouled oxygen sensor using generation-detection of oxygen

This chapter is reformatted from an article submitted to *Sensors and Actuators: B Chemical* entitled “In situ recalibration of a biofouled PoPD-coated oxygen sensor using generation-detection of oxygen on a microelectrode array” with manuscript ID SNB-D-17-01158 (accepted with major revision).

4.1 Abstract

Most chemical sensing development is based on newer platforms of technology. One of the practical limitations of sensors is their susceptibility to lose calibration when in use. Although some methods of in situ recalibration have been developed, sensors are normally recalibrated by extraction from the test environment and exposure to standards. In situ calibration has the advantage of avoiding extraction, which may cause tissue or sensor damage. It is well known that sensors lose calibration following in vivo implantation, and pre- and post-calibration methods have been used to compensate for the changes in sensitivity; we have recently reported and there is anecdotal evidence that the sensor sensitivity between the test environment and external calibration are not identical. Here we report the in situ recalibration of a biofouled oxygen sensor consisting of a polymer-coated microelectrode array. The sensitivity of a biofouled oxygen sensor decreases by 50% from the pre-calibrated sensitivity when incubated in fibrinogen solution. Our method of in situ recalibration predicts a new sensitivity for the biofouled oxygen sensor that is within 7% of the actual sensor sensitivity. This technique could provide a method to recalibrate implanted oxygen sensors for clinical or environmental applications.

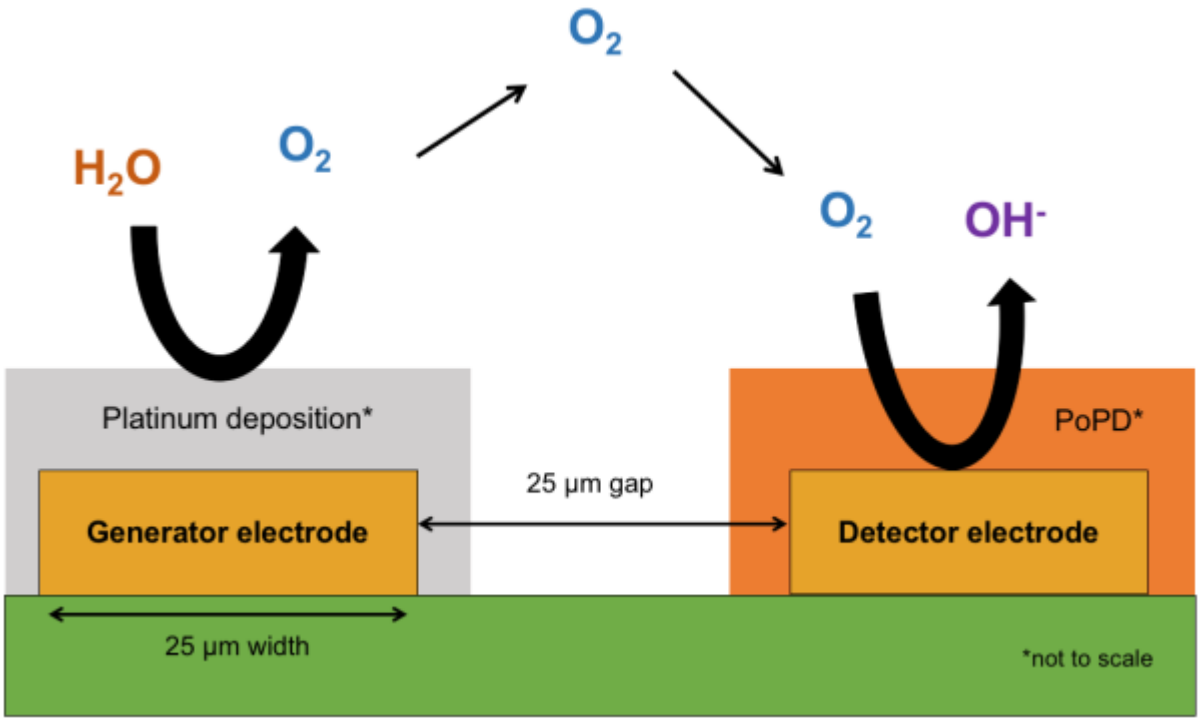

Graphical abstract: In situ recalibration method by generation-detection of oxygen to compensate for biofouled polymer-coated oxygen sensor on microelectrode arrays.

4.2 Introduction

Oxygen is of vital importance in biological systems and processes, ranging from environmental measurements to medical applications. Clinically, it has been shown that decreased oxygen levels in the brain are related to brain damage caused by trauma or ischemic stroke; patients with higher brain oxygen levels have a tendency to survive, while those with decreased brain oxygen do not. As stroke was the fifth leading cause of death in the U.S. in 2016, it is critically important to investigate methods to monitor the brain oxygen levels of these patients. There does not exist an absolute threshold value of brain oxygen level below which clinical intervention would be necessary because oxygen values vary significantly from patient to patient; these variations in one study were attributed to either differences in the probes or human error.[1] These oxygen variations are likely a result of a change in the sensitivity of the sensor following implantation.

In vivo sensors are typically calibrated pre- and post-implantation, and the sensor sensitivity while implanted is assumed to be the same as these calibrations. However, it is still unclear if in fact a post-calibration sensitivity is identical to that when the probe is implanted. There is some question whether using an in vitro calibration for determining in vivo measurements is accurate;[2] indeed some reports estimate that in vivo glucose sensors can be in error by as much as 100%.[3-4] In our previous work, we simulated an in vivo experiment which showed that the difference between in vitro and in vivo reported oxygen values could have a discrepancy of as much as 50%.[5] This could have major implications for all in vivo sensors, including those that sense oxygen. Therefore, it is imperative that an alternative method of calibration is investigated.

There have been few reports of in situ recalibration for in vivo sensors.[6-9] Typically, one-point calibrations are used for glucose and dopamine sensors with high selectivity and no background current at zero substrate concentration, while two-point calibrations are for sensors in which the background current is significant at zero substrate concentration.[10] Some researchers suggest that a one-point calibration could compensate for the immune response's effect on sensor sensitivity,[11] while others point out that multiple recalibrations may be necessary for long-term implanted sensors.[12] Using carbon fiber microelectrodes, Roberts et al designed a method to predict a new sensitivity for measuring dopamine, ascorbic acid, hydrogen peroxide, and pH shifts during in vivo experiments by utilizing the background charging current as a means of predicting sensitivity; this method performs comparably to traditional ex vivo calibration methods without the need to remove the working electrode from the in vivo test environment.[13]

All implanted devices are susceptible to the body's immune response, including wound healing, protein adsorption, and eventual encapsulation.[14-16] Protein adsorption to surfaces typically occurs quickly, and is usually followed by protein denaturation or conformational changes.[17-19] Protein adsorption affects the calibration of the sensor by altering the permeability of the membrane, hence hindering the analyte's ability to interact with the sensor surface.[20] Bovine serum albumin (BSA) and fibrinogen are typical proteins used as model biofoulants due to their high concentrations in blood plasma, and are both known to adsorb onto gold.[21-24] BSA has a molecular weight of approximately 66 kDa while fibrinogen is approximately 340 kDa.[25] Additionally, fibrinogen has been shown to readily and strongly adsorb onto negatively-polarized gold surfaces, which is the case in this work.[26]

Many methods have been employed in an attempt to minimize the effect of biofouling.[27] Liu et al. applied a BSA pretreatment (called "blocking," as a method to reduce nonspecific adsorption) to a carbon fiber electrode for in vivo dopamine sensing which showed similar results for pre- and post-calibration.[28] Ren et al. employed a nitric oxide generation/release scheme that actively inhibited biofouling for an amperometric oxygen sensing catheter;[29] a similar method has been employed for use with an in vivo glucose sensor.[30] Yang et al. noted that by coating a zwitterionic poly(carboxybetaine) hydrogel onto a glucose sensor, blood-materials interactions were minimized and the life of the sensor was extended.[31] Poly-o-phenylenediamine (PoPD) has been used as a protective coating for many types of sensors, including glucose,[32-36] hydrogen peroxide,[37-42] oxygen,[43-45] and others.[46-51] While there has been extensive research of coatings used to minimize biofouling, some researchers have concluded that a completely anti-fouling coating is unlikely to ever be realized.[52]

In situ oxygen generation has been developed but not used for in situ recalibration of oxygen sensors. Sherman et al. were able to electrochemically produce and quantify oxygen with their dual working electrode collector-generator cell using fluorine doped tin oxide electrodes.[53] Sun et al. immobilized two different enzymes onto GC/AuNP electrodes to take advantage of the enzymes' reactions that generate oxygen as a coreactant, which then acted as a signal amplifier in their electrochemiluminescent detection of carcinoembryonic antigen.[54] Yang et al. developed a porous cobalt catalyst that can be used for both hydrogen and oxygen generation depending on the potential applied, which could be of great importance for use in renewable energy devices.[55] Xu et al. designed a nanofluidic device with an embedded microband electrode that can generate oxygen; generated oxygen is monitored and quantified using fluorescence and pH relationships.[56]

While these studies have successfully generated oxygen in situ, we present the first study of an in situ recalibrated oxygen sensor using microelectrode arrays.

4.3 Materials and Methods

4.3.1 In Situ Recalibration Method

In a previous study, an in situ recalibration method was described for an oxygen sensor using macroelectrodes;[57] this work applies that same in situ recalibration method to microelectrode arrays. Microelectrode arrays offer the advantage of individually addressable electrodes, which allows for precise electrodeposition and the ability to utilize distinct electrodes for different purposes; for example, one can apply a constant potential at one electrode to generate oxygen, while obtaining cyclic voltammetry data on a neighboring electrode to detect the increase in oxygen concentration. Microelectrodes are also a more viable option when studying possible in vivo applications because their smaller size is likely to cause less tissue trauma upon implantation.

Electrochemical oxygen sensors function by measuring the steady-state diffusion limiting current, i_{DL}, which is proportional to the concentration of oxygen in the test environment, C_s, and the sensor sensitivity, S:

$$i_{DL} = SC_S \tag{1}$$

The sensitivity of the sensor is determined by two factors: permeability of the membrane, P_m, and thickness of the membrane, b.

$$S = \frac{nFP_m}{b} \tag{2}$$

Biofouling changes the properties of the membrane, causing a change in sensor sensitivity from an initial value of S_1 to an unknown value of S_2. Currently, the only way to

determine S_2 is to remove the sensor from the test environment and perform a calibration. However, by introducing a second oxygen-generating electrode (GE), external to the membrane, oxygen can be generated without the need to remove the probe. To recalibrate the sensor and find S_2, the GE is poised at a potential such that water is oxidized to oxygen. This will cause a local change in the concentration profile which causes an increase in the steady-state concentration of oxygen at the surface of the membrane ΔC_S at the surface of the oxygen sensor's membrane, provided it is close enough to the GE:

$$i_{GE} = \xi(\Delta C_S) \tag{3}$$

where i_{GE} is the steady-state current value at the GE, and ξ is a proportionality constant specific to the geometry of the electrode.[57] The local change in concentration of oxygen will also cause a change in diffusion limiting current, Δi_{DL}, as shown in Equation (4):

$$\Delta i_{DL} = S(\Delta C_S) \tag{4}$$

To determine ξ, an oxygen calibration curve is constructed, the slope being S_1 for the electrode; then, oxygen generation-detection is performed to determine i_{GE} and the change in detector limiting current, Δi_{DL}; then, knowing Δi_{DL} and S_1, ΔC_S can be found using Equation (4); finally, one can solve for ξ by using Equation (3). An example illustrating this method is shown in Fig. 4.1. Once ξ is known, if a sensitivity change then occurs, such as a biofouling event, the new sensitivity value S_2 can be determined using Equation (5):

$$\frac{\Delta i_{DE}}{i_{GE}} = \frac{S_2}{\xi} \tag{5}$$

4.3.2 Reagents

O-phenylenediamine (oPD) monomer (Sigma, St. Louis, MO), bovine albumin (Amresco, Solon, OH), bovine fibrinogen (Alfa Aesar, Ward Hill, MA), phosphate buffered saline tablets (PBS) (EMD Millipore, Billerica, MA), K_2PtCl_4 salt (Sigma-Aldrich, St. Louis,

MO) were obtained. Solutions of oPD monomer (300 mM) were prepared in 10 mM PBS. Unless otherwise stated, experiments were performed in PBS solution, pH 7.4 (140 mM NaCl, 10 mM phosphate buffer, 3 mM KCl). A CH Instruments 1030A potentiostat, Ag/AgCl (in sat'd KCl) reference electrode, and platinum flag counter electrode were used in all experiments.

4.3.3 Electrode Preparation

Microelectrode arrays (MEAs) were constructed on silicon wafer substrate via photolithography. Microelectrodes used in the study consisted of an array of sixteen interdigitated microbands on a 1 inch x 1 inch silicon substrate. Each of the bands were 2 mm long, 25 µm wide and the gap between two adjacent bands was 25 µm. The microband arrays were constructed by applying UV photolithography technique on the metallized layer of 10 nm titanium/500 nm gold on the silicon wafer. The areas except the exposed bands on the substrate were protected with an insulating layer of benzocyclobutane. The finished MEA chip was cleaned via oxygen plasma and stored in deionized water. Polymerization solutions of 300 mM oPD monomer were prepared by dissolving in 10 mM PBS and sonicating for 30 minutes; PoPD-coated gold microband electrodes were produced by applying a constant potential of +0.9 V (vs Ag/AgCl in sat'd KCl reference) for 30 minutes.[58] Generator electrodes (GE) were prepared by electrodepositing platinum on top of the gold microband electrode: 3 successive depositions in 20 mM K_2PtCl_4 in 1 M $HClO_4$ by applying a constant potential of -0.1 V vs Ag/AgCl in sat'd KCl reference for a pulse width of 5 seconds each.[59]

4.3.4 Oxygen Calibration Curves

The test solution (either control electrolyte PBS or PBS/biofoulant solution) was purged of oxygen by bubbling nitrogen and allowing ambient oxygen to re-dissolve. The dissolved oxygen concentration was measured using a YSI Pro20 oxygen meter (Yellow Springs, OH).

Cyclic voltammograms (CVs) of increasing dissolved oxygen concentration were obtained at PoPD-coated microelectrodes by sweeping the potential from 0 V to -1.0 V vs Ag/AgCl in sat'd KCl reference electrode. Calibration curves were then constructed by plotting the resulting current value at -0.6 V vs Ag/AgCl in sat'd KCl reference electrode versus the dissolved oxygen concentration; sensor sensitivity to oxygen is taken as the slope of this line.

4.3.5 Determination of ξ and Recalibration of Sensitivity

A cyclic voltammogram (CV) was taken on the DE from 0 to -1.0 V vs Ag/AgCl in sat'd KCl reference electrode to reduce the ambient oxygen. Then, the GE was poised at a constant potential of +1.4 V vs Ag/AgCl in sat'd KCl reference electrode to generate oxygen from water; simultaneously, another CV was taken on the DE from 0 to -1.0 V vs Ag/AgCl in sat'd KCl reference electrode to reduce and detect the generated and endogenous oxygen. This is illustrated in Fig. 4.1. The change in current at the DE, Δi_{DL}, was obtained by taking the difference in current response at -0.6 V from the resulting CVs and the current at the GE, i_{GE}. Values were then used along with the sensitivity, S_1, from Section 4.2.4, to calculate the ξ term. Once ξ was known, another generation-detection experiment was performed while the MEA was incubated in test solution containing biofoulant, and a new sensitivity, S_2, was predicted for the biofouled electrode.

4.4 Results and Discussion

4.4.1 Electrodeposition of Platinum on a MEA

An alternative GE material to gold was necessary due to the high positive potential needed to generate O_2. An over coating of platinum was selected because it offers the advantage electrocatalytic activity. Investigations determining an adequate method to deposit platinum onto the gold microband electrode commenced. After many trials of various procedures, the method

described in Section 4.2.3 was determined to produce the most robust and repeatable platinum deposition that generates sufficient amounts of O_2, without dissolution of the GE. A diagram of such a Pt-deposited gold microband on the MEA is presented in Fig. 4.2.

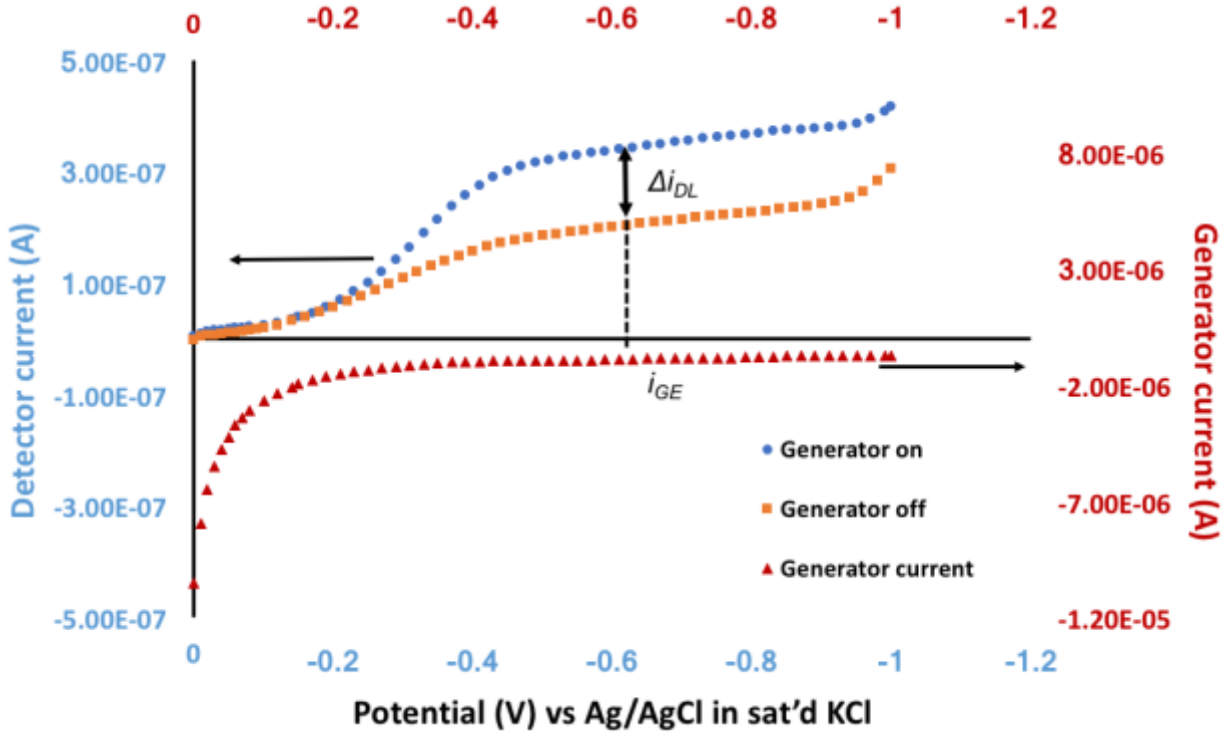

Figure 4.1 Generation-detection of oxygen data example for in situ recalibration. CVs are obtained on the DE both with the GE "on" (blue circles) and "off" (orange squares), and the GE while "on" (red triangles). Δi_{DE} is the difference between current values of "Generator on" and "Generator off" for the DE, and i_{GE} is the current at the GE of "Generator on," both taken at -0.6 V vs Ag/AgCl in sat'd KCl reference electrode. The left axis corresponds to the DE for both "Generator on" and "Generator off" CVs; the right axis corresponds to the CV at the GE while it's poised at +1.4 V (vs Ag/AgCl in sat'd KCl reference).

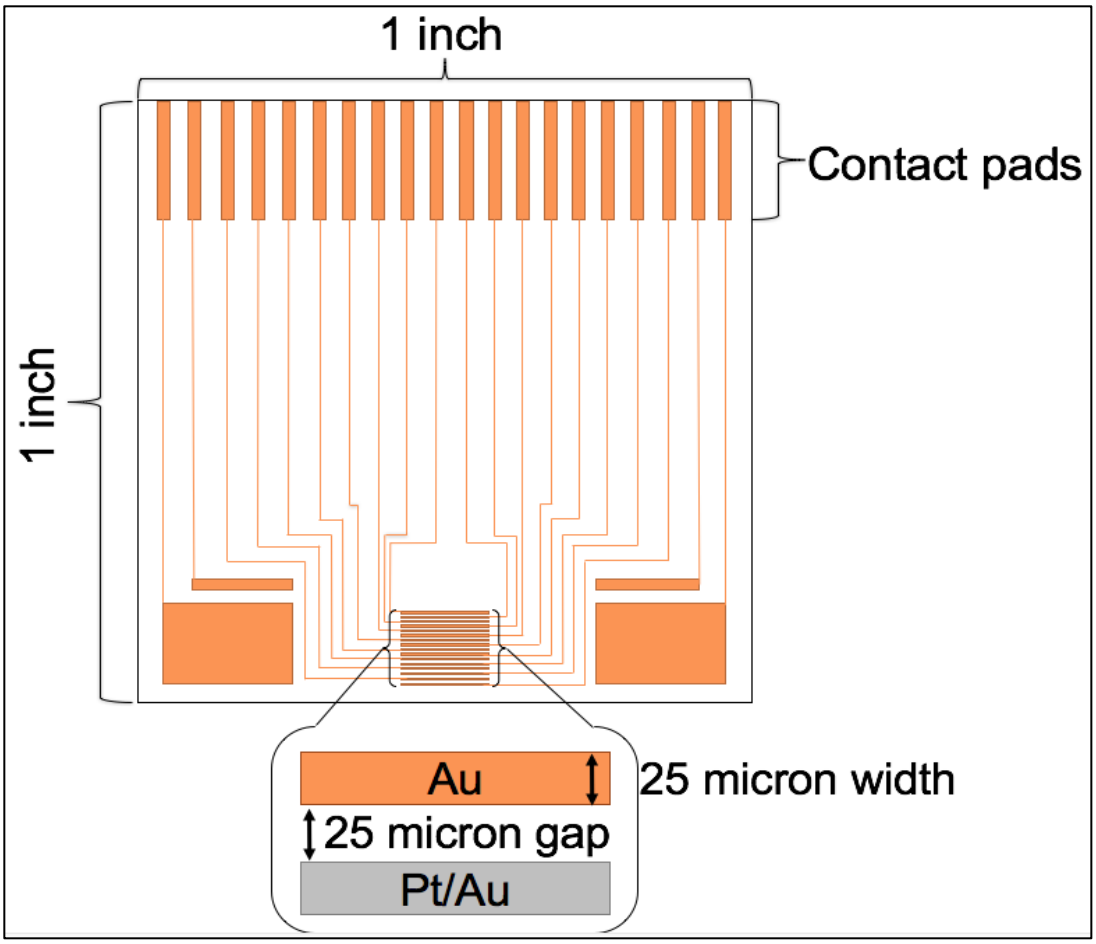

Figure 4.2 Diagram of the MEA chip showing dimension schematics. Zoomed in section shows the dimensions of the microbands, as well as the Pt deposition on Au.

4.4.2 Oxygen Sensor Response with Exposure to BSA

BSA is commonly used as a model foulant in biofouling studies. We showed in a previous study that BSA initially fouls substantially, followed by protein desorption from the sensor surface as is evident by sensor sensitivity returning to a similar pre-fouled value.[5] This work began by intentionally fouling the PoPD-coated microband electrodes with 6 g/L BSA solution and monitoring the oxygen sensitivity over time. Unlike our previous work which exhibited dramatic decrease in sensitivity initially, Fig. 4.3 indicates that BSA did not adsorb to the PoPD-coated oxygen sensor, as the sensor sensitivity to oxygen did not appreciably change over time. It can be concluded therefore that BSA is not a primary biofoulant for gold microband electrodes as it was for the gold macrodisk electrode counterparts. The reason for this is unknown ostensibly; the only difference between the two are the edge effects that are more pronounced in microelectrodes.

4.4.3 Oxygen Sensor Response with Exposure to Fibrinogen

Fibrinogen has been shown in our previous work to be a substantial fouling protein.[5] Oxygen calibration curves were obtained on the PoPD-coated microelectrode in control electrolyte (10 mM PBS), immediately following incubation in 3 g/L fibrinogen solution, and after one day of incubation in fibrinogen solution. These calibration curves are presented in Fig. 4.4. In control electrolyte, the PoPD-coated microelectrode exhibited an oxygen sensitivity of 33.0 nA/ppm. Upon immediate incubation in fibrinogen solution, the oxygen sensitivity decreased to a value of 24.7 nA/ppm, and after one day of incubation it further declined to a value of 22.0 nA/ppm. This follows the trend expected based on our previous study, which showed that with fibrinogen incubation, oxygen sensitivity is suppressed and remains suppressed over time.[5]

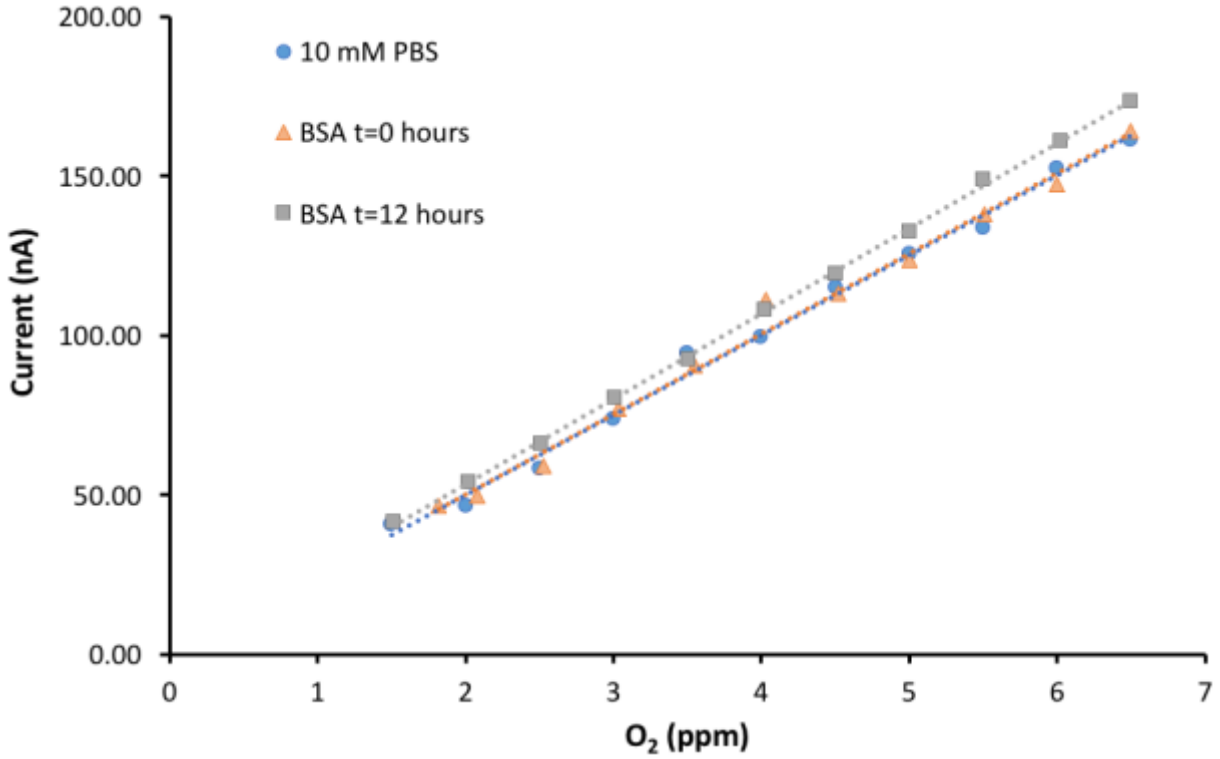

Figure 4.3 Oxygen calibration curves for a PoPD-coated electrode (n=1) in control electrolyte (10 mM PBS, blue circles), and while incubated in BSA solution immediately following incubation (orange triangles) and after 12 hours of incubation (gray squares); O_2 current value taken at -0.6 V vs Ag/AgCl in sat'd KCl reference.

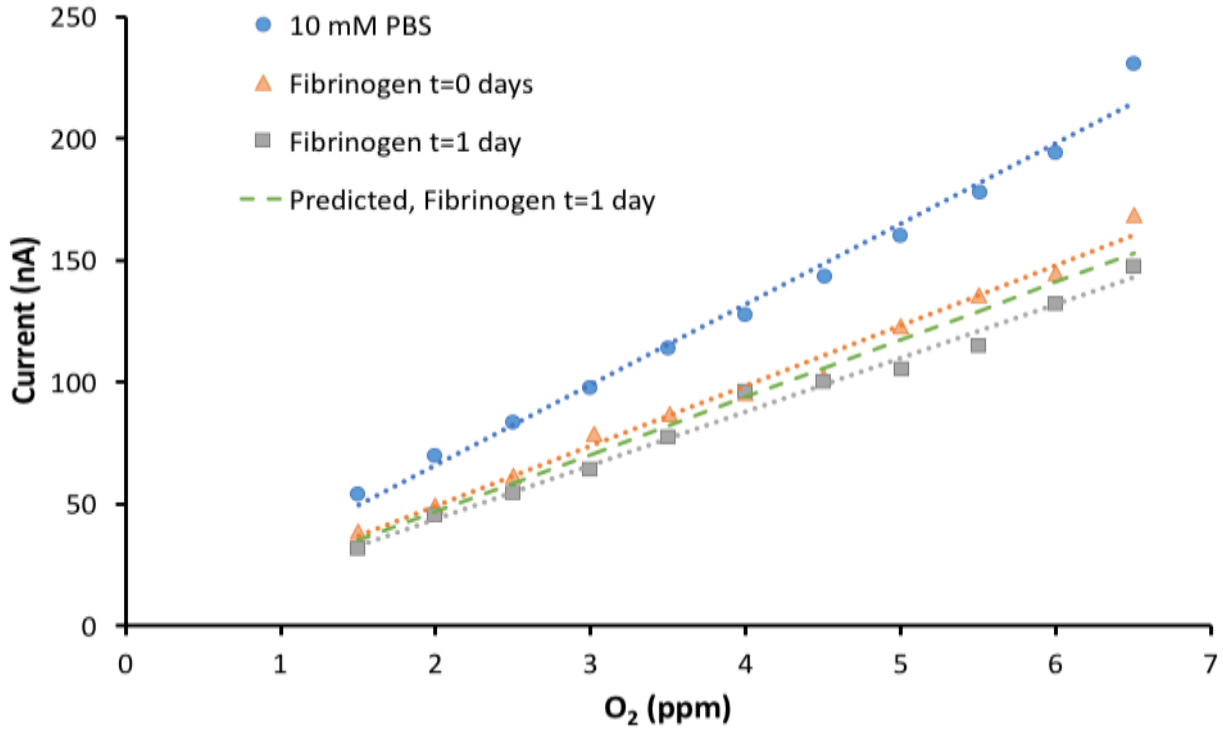

Figure 4.4 Oxygen calibration curves for a PoPD-coated electrode (n=1) in control electrolyte (10 mM PBS, blue circles), and while incubated in fibrinogen solution immediately following incubation (orange triangles) and after 1 day of incubation (gray squares). The predicted sensitivity after 1 day of fibrinogen incubation is also plotted (green dashed line); O_2 current value taken at -0.6 V vs Ag/AgCl in sat'd KCl reference.

4.4.4 In Situ Recalibration

Oxygen generation-detection experiments were then performed on the biofouled PoPD-coated microelectrode as described in Section 4.2.5. Using the ξ value calculated from Equation (3) for the bare gold microelectrode in control electrolyte, a new oxygen sensitivity was predicted for the biofouled electrode after one day of incubation (Table 4.1). Since all electrodes behave differently, each PoPD-coated electrode was treated individually to prove the efficacy of the method. Table 4.1 describes the experimental values for the three individual electrodes, including the distinct ξ values, and sensitivities obtained in control electrolyte (10 mM PBS) and 3 g/L fibrinogen solution both immediately following incubation and after 1 day of incubation. In addition, using data obtained during Generation-Detection of Oxygen experiments (Section 2.5), predicted sensitivities were calculated for each of the biofouled electrodes after 1 day of incubation in fibrinogen solution. The predicted sensitivity values for all 3 electrodes are in agreement with the true sensitivity values (fibrinogen t=1 day) within an error of 7%. In addition, the Pt/Au GE is able to generate O_2, even when incubated in the same biofouling solution; this shows that the ability for the GE to generate O_2 is unaffected by biofouling.

It has been stated previously that even a slight change in calibrated sensitivity of an oxygen sensor can cause a significant discrepancy in measured oxygen values. For example, as can be seen in Fig. 4.4, if the sensor sensitivity obtained in control electrolyte (33.0 nA/ppm) is used to measure dissolved oxygen when incubated in fibrinogen solution, a current response of 150 nA leads to a reported oxygen value of approximately 4.51 ppm; using the actual sensor sensitivity (22.0 nA/ppm), the same current response of 150 nA, the reported oxygen value would be approximately 6.50 ppm. While the percent error between sensor sensitivity obtained in control electrolyte and biofoulant solution is 50%, this induces a total error in reported oxygen

values of 31%. If the recalibrated sensitivity (23.5 nA/ppm) is used, a current response of 150 nA would result in a reported oxygen value of 6.38 ppm O_2 (an error of 1.85%). Most researchers would use the sensitivity value for control electrolyte, assuming that it remains the same when incubated in the test environment; our results show that the sensitivity does change significantly when incubated in a protein solution, which would lead to inaccurate reported oxygen values. However, using our method of in situ recalibration, the biofouled sensor sensitivity is accounted for, leading to more accurate reported oxygen values. This could have significant implications for in vivo sensors used in clinical settings.

		Experimental O_2 Sensitivity (nA/ppm)			Predicted O_2 Sensitivity (nA/ppm)	
Electrode	ξ (ppm/nA)	Control electrolyte	Fibrinogen, t=0	Fibrinogen, t=1 day	Fibrinogen, t=1 day	Percent error (%)
1	173	41.4	32.2	34.0	31.9	6.01
2	198	33.6	26.4	28.0	29.7	6.25
3	141	33.0	24.7	22.0	23.5	7.04

Table 4.1 Calibration values for three individual PoPD-coated electrodes incubated in fibrinogen solution

4.5 Conclusion

This work shows the efficacy of an in situ recalibration method of a biofouled oxygen sensor using polymer-coated microelectrode arrays. Each sensor behaves differently and has its own individual sensitivity and therefore should be treated independently.[13] Using this method of in situ recalibration, biofouled electrodes were recalibrated to within 7% error of the actual calibration when incubated in fibrinogen solution. However, this method has its limitations and cannot account for excessive fouling (6 g/L concentration fibrinogen, nearly double the normal endogenous concentration in blood), which caused a complete suppression of oxygen sensitivity

(data not shown). There are a few possibilities for why this method is unable to achieve 0% error. It is possible that the electrodes become extremely fouled, leading to the detector electrode being unable to detect the change in O_2 concentration. This could be due to O_2 either not being generated at the GE; or, if O_2 is generated at the GE, the O_2 not being able to diffuse and be detected by the DE. The data suggest that it is likely not the former, as generator currents remain the same order of magnitude as the control, before fouling. It is feasible that the O_2 generated at the GE cannot diffuse through the biofilm either on the GE, the DE, the space between the GE and DE, or some combination of all three. A method to investigate this is by using scanning electrochemical microscopy, SECM. This technique would allow investigation as to which microenvironment is causing the decreased change in DE current.

As all generate-detect experiments were done in ambient O_2, the biofilm layer could already be saturated with O_2, and therefore generating additional O_2 will not have an impact on the DE current. A way to test this would be to purge the biofilm layer of O_2 by keeping the DE on closed circuit at -0.6 V, while the bulk solution is also purged with N_2; if the biofilm is O_2 saturated then over time, the DE current should decrease to a constant value as all O_2 is reduced in the layer.

Another possibility is that the generated O_2 is able to diffuse through the unsaturated biofilm, but diffusion is much slower, too slow in fact to see the apparent change in DE current on our experimental time scale. A method to investigate this possibility would be to use electrochemical time of flight, ETOF. Using ETOF, the diffusion coefficient of O_2 through the biofilm could be determined. This would give information about how quickly generated O_2 could diffuse through the biofilm and be detected at the DE. Chronoamperometry could also be used instead of cyclic voltammetry, in which the current at steady-state could be used in calculating xi

and predicting a new sensitivity for the oxygen sensor, since chronoamperometry would not have the added disadvantage of being dependent on the duration of the experiment.

4.6 Acknowledgments

The authors acknowledge financial support from the Arkansas Biosciences Institute, the major research component of the Arkansas Tobacco Settlement Proceeds Act of 2000. We are also grateful to Errol Porter of the High Density Electronics Center at the University of Arkansas for assistance with microelectrode array fabrication, and Alda Diaz Perez for sample preparation assistance.

4.7 References

1. Nozue, M.; Lee, I.; Yuan, F.; Teicher, B. A.; Brizel, D. M.; Dewhirst, M. W.; Milross, C. G.; Milas, L.; Song, C. W.; Thomas, C. D.; Guichard, M.; Evans, S. M.; Koch, C. J.; Lord, E. M.; Jain, R. K.; Suit, H. D., Interlaboratory variation in oxygen tension measurement by Eppendorf "Histograph" and comparison with hypoxic marker. *Journal of surgical oncology* **1997,** *66* (1), 30-8.

2. Koschwanez, H. E.; Reichert, W. M., In vitro, in vivo and post explantation testing of glucose-detecting biosensors: Current methods and recommendations. *Biomaterials* **2007,** *28* (25), 3687-3703.

3. Gerritsen, M.; Jansen, J. A.; Lutterman, J. A., Performance of subcutaneously implanted glucose sensors for continuous monitoring. *Netherlands Journal of Medicine* **1999,** *54* (4), 167-179.

4. Velho, G.; Froguel, P.; Thevenot, D. R.; Reach, G., Strategies for calibrating a subcutaneous glucose sensor. *Biomedica Biochimica Acta* **1989,** *48* (11-12), 957-64.

5. Patrick, M. M.; Grillot, J. M.; Derden, Z. M.; Paul, D. W., Long-term drifts in sensitivity caused by biofouling of an amperometric oxygen sensor. *Electroanalysis* **2017,** *29* (4), 998-1005.

6. Csoeregi, E.; Quinn, C. P.; Schmidtke, D. W.; Lindquist, S.-E.; Pishko, M. V.; Ye, L.; Katakis, I.; Hubbell, J. A.; Heller, A., Design, Characterization, and One-Point in vivo Calibration of a Subcutaneously Implanted Glucose Electrode. *Anal. Chem.* **1994,** *66* (19), 3131-8.

7. Jeong, R.-A.; Hwang, J. Y.; Joo, S.; Chung, T. D.; Park, S.; Kang, S. K.; Lee, W.-Y.; Kim, H. C., In vivo calibration of the subcutaneous amperometric glucose sensors using a non-enzyme electrode. *Biosens. Bioelectron.* **2003,** *19* (4), 313-319.

8. Aussedat, B.; Thome-Duret, V.; Reach, G.; Lemmonier, F.; Klein, J. C.; Hu, Y.; Wilson, G. S., A user-friendly method for calibrating a subcutaneous glucose sensor-based hypoglycaemic alarm. *Biosensors & bioelectronics* **1997,** *12* (11), 1061-71.

9. Von Woedtke, T.; Rebrin, K.; Fischer, U.; Abel, P.; Wilke, W.; Vogt, L.; Albrecht, G., In situ calibration of implanted electrochemical glucose sensors. *Biomedica Biochimica Acta* **1989,** *48* (11-12), 943-52.

10. Govindarajan, S.; Manshian, B. B., Implantable electrochemical biosensors: a perspective. *Pan Stanford Series on Biomedical Nanotechnology* **2013,** *3* (Biomedical Nanosensors), 349-374.

11. Frost, M.; Meyerhoff, M. E., In Vivo Chemical Sensors: Tackling Biocompatibility. *Anal. Chem.* **2006,** *78* (21), 7370-7377.

12. Renard, E.; Costalat, G.; Chevassus, H.; Bringer, J., Artificial β-cell: clinical experience toward an implantable closed-loop insulin delivery system. *Diabetes & Metabolism* **2006,** *32* (5, Pt. 2), 497-502.

13. Roberts, J. G.; Toups, J. V.; Eyualem, E.; McCarty, G. S.; Sombers, L. A., In Situ Electrode Calibration Strategy for Voltammetric Measurements In Vivo. *Anal. Chem. (Washington, DC, U. S.)* **2013,** *85* (23), 11568-11575.

14. Klueh, U.; Liu, Z.; Ouyang, T.; Cho, B.; Feldman, B.; Henning Timothy, P.; Kreutzer, D., Blood-induced interference of glucose sensor function in vitro: implications for in vivo sensor function. *J Diabetes Sci Technol* **2007,** *1* (6), 842-9.

15. Ratner, B. D.; Bryant, S. J., Biomaterials: Where we have been and where we are going. *Annual Review of Biomedical Engineering* **2004,** *6*, 41-75.

16. Anderson, J. M.; Rodriguez, A.; Chang, D. T., Foreign body reaction to biomaterials. *Semin. Immunol.* **2008,** *20* (2), 86-100.

17. Collyer, S.; Davis, F.; Lucke, A.; Stirling, C. J. M.; Higson, S. P. J., An investigation into outer-surface biofouling and electrode passivation effects on gold electrodes modified with calix[4]resorcinarenetetrathiol and a PEG derivative on exposure to whole human blood. *Electroanalysis* **2004,** *16* (4), 275-281.

18. Higson, S. P. J.; Desai, M. A.; Ghosh, S.; Christie, I.; Vadgama, P., Amperometric enzyme electrode biofouling and passivation in blood: Characterization of working electrode polarization and inner membrane effects. *J. Chem. Soc., Faraday Trans.* **1993,** *89* (15), 2847-51.

19. Sadana, A., Protein adsorption and inactivation on surfaces. Influence of heterogeneities. *Chemical Reviews (Washington, DC, United States)* **1992,** *92* (8), 1799-818.

20. Barfidokht, A.; Gooding, J. J., Approaches Toward Allowing Electroanalytical Devices to be Used in Biological Fluids. *Electroanalysis* **2014,** *26* (6), 1182-1196.

21. Moulton, S. E.; Barisci, J. N.; Bath, A.; Stella, R.; Wallace, G. G., Investigation of protein adsorption and electrochemical behavior at a gold electrode. *Journal of Colloid and Interface Science* **2003,** *261* (2), 312-319.

22. Moulton, S. E.; Barisci, J. N.; Bath, A.; Stella, R.; Wallace, G. G., Studies of double layer capacitance and electron transfer at a gold electrode exposed to protein solutions. *Electrochimica Acta* **2004,** *49* (24), 4223-4230.

23. Ying, P.; Viana, A. S.; Abrantes, L. M.; Jin, G., Adsorption of human serum albumin onto gold: a combined electrochemical and ellipsometric study. *Journal of Colloid and Interface Science* **2004,** *279* (1), 95-99.

24. Szott, L. M.; Horbett, T. A., Mechanisms of the foreign body response to RFGD plasma-generated PEO-like films. *ACS Symposium Series* **2012,** *1120* (Proteins at Interfaces III), 321-337.

25. Glomm, W. R.; Halskau, O., Jr.; Hanneseth, A.-M. D.; Volden, S., Adsorption Behavior of Acidic and Basic Proteins onto Citrate-Coated Au Surfaces Correlated to Their Native Fold, Stability, and pI. *Journal of Physical Chemistry B* **2007,** *111* (51), 14329-14345.

26. Dargahi, M.; Konkov, E.; Omanovic, S., Influence of Surface Charge/Potential of a Gold Electrode on the Adsorptive/Desorptive Behaviour of Fibrinogen. *Electrochimica Acta* **2015,** *174*, 1009-1016.

27. Hanssen, B. L.; Siraj, S.; Wong, D. K. Y., Recent strategies to minimise fouling in electrochemical detection systems. *Reviews in Analytical Chemistry* **2016,** *35* (1), 1-28.

28. Liu, X.; Zhang, M.; Xiao, T.; Hao, J.; Li, R.; Mao, L., Protein Pretreatment of Microelectrodes Enables in Vivo Electrochemical Measurements with Easy Precalibration and Interference-Free from Proteins. *Analytical Chemistry (Washington, DC, United States)* **2016,** *88* (14), 7238-7244.

29. Ren, H.; Coughlin, M. A.; Major, T. C.; Aiello, S.; Rojas Pena, A.; Bartlett, R. H.; Meyerhoff, M. E., Improved in Vivo Performance of Amperometric Oxygen (PO2) Sensing Catheters via Electrochemical Nitric Oxide Generation/Release. *Analytical Chemistry (Washington, DC, United States)* **2015,** *87* (16), 8067-8072.

30. Wolf, A. K.; Qin, Y.; Major, T. C.; Meyerhoff, M. E., Improved thromboresistance and analytical performance of intravascular amperometric glucose sensors using optimized nitric oxide release coatings. *Chinese Chemical Letters* **2015,** *26* (4), 464-468.

31. Yang, W.; Xue, H.; Carr, L. R.; Wang, J.; Jiang, S., Zwitterionic poly(carboxybetaine) hydrogels for glucose biosensors in complex media. *Biosens. Bioelectron.* **2011,** *26* (5), 2454-2459.

32. Rothwell, S. A.; Killoran, S. J.; O'Neill, R. D., Enzyme immobilization strategies and electropolymerization conditions to control sensitivity and selectivity parameters of a polymer-enzyme composite glucose biosensor. *Sensors* **2010,** *10*, 6439-6462.

33. Dixon, B. M.; Lowry, J. P.; O'Neill, R. D., Characterization in vitro and in vivo of the oxygen dependence of an enzyme/polymer biosensor for monitoring brain glucose. *J. Neurosci. Methods* **2002,** *119* (2), 135-142.

34. Lowry, J. P.; McAteer, K.; El Atrash, S. S.; Duff, A.; O'Neill, R. D., Characterization of Glucose Oxidase-Modified Poly(phenylenediamine)-Coated Electrodes in vitro and in vivo: Homogeneous Interference by Ascorbic Acid in Hydrogen Peroxide Detection. *Anal. Chem.* **1994,** *66* (10), 1754-61.

35. Turkmen, E.; Bas, S. Z.; Gulce, H.; Yildiz, S., Glucose biosensor based on immobilization of glucose oxidase in electropolymerized poly(o-phenylenediamine) film on platinum nanoparticles-polyvinylferrocenium modified electrode. *Electrochimica Acta* **2014,** *123*, 93-102.

36. Kealy, J.; Bennett, R.; Lowry John, P., Simultaneous recording of hippocampal oxygen and glucose in real time using constant potential amperometry in the freely-moving rat. *Journal of neuroscience methods* **2013,** *215* (1), 110-20.

37. Ariffin, A. A.; O'Neill, R. D.; Yahya, M. Z. A.; Zain, Z. M., Electropolymerization of ortho-phenylenediamine and its use for detection on hydrogen peroxide and ascorbic acid by electrochemical impedance spectroscopy. *International Journal of Electrochemical Science* **2012,** *7* (10), 10154-10163.

38. Killoran, S. J.; O'Neill, R. D., Characterization of permselective coatings electrosynthesized on Pt-Ir from the three phenylenediamine isomers for biosensor applications. *Electrochimica Acta* **2008,** *53* (24), 7303-7312.

39. Rothwell, S. A.; Killoran, S. J.; Neville, E. M.; Crotty, A. M.; O'Neill, R. D., Poly(o-phenylenediamine) electrosynthesized in the absence of added background electrolyte provides a new permselectivity benchmark for biosensor applications. *Electrochem. Commun.* **2008,** *10* (7), 1078-1081.

40. Rothwell, S. A.; McMahon, C. P.; O'Neill, R. D., Effects of polymerization potential on the permselectivity of poly(o-phenylenediamine) coatings deposited on Pt-Ir electrodes for biosensor applications. *Electrochimica Acta* **2009,** *55* (3), 1051-1060.

41. Zhai, W.; Tian, X.; Yan, Y.; Xu, Y.; Zhao, Y.; Liu, Y., Preparation and characterization of a poly-o-phenylenediamine film modified glassy carbon electrode as a H2O2 sensor. *Canadian Journal of Chemistry* **2013,** *91* (11), 1077-1084.

42. O'Brien, K. B.; Killoran, S. J.; O'Neill, R. D.; Lowry, J. P., Development and characterization in vitro of a catalase-based biosensor for hydrogen peroxide monitoring. *Biosens. Bioelectron.* **2007,** *22* (12), 2994-3000.

43. Bolger, F. B.; Bennett, R.; Lowry, J. P., An in vitro characterisation comparing carbon paste and Pt microelectrodes for real-time detection of brain tissue oxygen. *Analyst (Cambridge, U. K.)* **2011,** *136* (19), 4028-4035.

44. Li, Y. J.; Lenigk, R.; Wu, X. Z.; Gruendig, B.; Dong, S. J.; Renneberg, R., Investigation of oxygen and hydrogen peroxide reduction on platinum particles dispersed on poly(o-phenylenediamine) film-modified glassy carbon electrodes. *Electroanalysis* **1998,** *10* (10), 671-676.

45. Premkumar, J.; Ramaraj, R., Permeation and electrocatalytic reduction of oxygen by poly(o-phenylenediamine) incorporated into Nafion film. *Journal of Applied Electrochemistry* **1996,** *26* (7), 763-766.

46. Kong, L.; Jiang, X.; Zeng, Y.; Zhou, T.; Shi, G., Molecularly imprinted sensor based on electropolmerized poly(o-phenylenediamine) membranes at reduced graphene oxide modified electrode for imidacloprid determination. *Sensors and Actuators, B: Chemical* **2013,** *185*, 424-431.

47. Kong, Y.; Shan, X.; Ma, J.; Chen, M.; Chen, Z., A novel voltammetric sensor for ascorbic acid based on molecularly imprinted poly(o-phenylenediamine-co-o-aminophenol). *Analytica Chimica Acta* **2014,** *809*, 54-60.

48. Liu, X.; Zhu, H.; Yang, X., An electrochemical sensor for dopamine based on poly(o-phenylenediamine) functionalized with electrochemically reduced graphene oxide. *RSC Advances* **2014,** *4* (8), 3706-3712.

49. Zhang, L.; Lian, J., The electrochemical polymerization of o-phenylenediamine on l-tyrosine functionalized glassy carbon electrode and its application. *Journal of Solid State Electrochemistry* **2008,** *12* (6), 757-763.

50. Wynne, A. M.; Reid, C. H.; Finnerty, N. J., In vitro characterization of ortho phenylenediamine and Nafion-modified Pt electrodes for measuring brain nitric oxide. *Journal of Electroanalytical Chemistry* **2014,** *732*, 110-116.

51. Brown, F. O.; Finnerty, N. J.; Lowry, J. P., Nitric oxide monitoring in brain extracellular fluid: characterisation of Nafion-modified Pt electrodes in vitro and in vivo. *Analyst (Cambridge, U. K.)* **2009,** *134* (10), 2012-2020.

52. Klueh, U., Analysis: on the path to overcoming glucose-sensor-induced foreign body reactions. *Journal of diabetes science and technology* **2013,** *7* (2), 452-4.

53. Sherman, B. D.; Sheridan, M. V.; Dares, C. J.; Meyer, T. J., Two Electrode Collector-Generator Method for the Detection of Electrochemically or Photoelectrochemically Produced O2. *Analytical Chemistry (Washington, DC, United States)* **2016,** *88* (14), 7076-7082.

54. Sun, A.; Qi, Q.; Wang, X.; Bie, P., A novel electrochemiluminescent detection of protein biomarker using L-cysteine and in situ generating coreactant for signal amplification. *Sensors and Actuators, B: Chemical* **2014,** *192*, 685-690.

55. Yang, Y.; Fei, H.; Ruan, G.; Tour, J. M., Porous Cobalt-Based Thin Film as a Bifunctional Catalyst for Hydrogen Generation and Oxygen Generation. *Advanced Materials (Weinheim, Germany)* **2015,** *27* (20), 3175-3180.

56. Xu, W.; Foster, E.; Ma, C.; Bohn, P. W., On-demand in situ generation of oxygen in a nanofluidic embedded planar microband electrochemical reactor. *Microfluidics and Nanofluidics* **2015,** *19* (5), 1181-1189.

57. Johnson, C. D.; Paul, D. W., In situ calibrated oxygen electrode. *Sensors and Actuators, B: Chemical* **2005,** *105* (2), 322-328.

58. Sardesai, N. P.; Ganesana, M.; Karimi, A.; Leiter, J. C.; Andreescu, S., Platinum-Doped Ceria Based Biosensor for in Vitro and in Vivo Monitoring of Lactate during Hypoxia. *Analytical Chemistry (Washington, DC, United States)* **2015,** *87* (5), 2996-3003.

59. Kawai, M.; Fukumuro, N.; Yae, S.; Matsuda, H., Electrochemical deposition of Pt particles from hexachloroplatinate(IV) ion and tetrachloroplatinate(II) ion solutions. *ECS Transactions* **2010,** *25* (33, Student Poster (General)--216th ECS Meeting, 2009), 117-123.

5. Conclusions and Future Work

5.1 Conclusions

The investigations described in this dissertation contribute to the field of in vivo oxygen sensors. Until these works, in vivo sensors operated under the assumption that in vitro sensor calibration remains valid when implanted in vivo. Studies described here demonstrate not only that this assumption is not valid, but also provide quantification of the change in sensor sensitivity when incubated under ex vivo conditions. Furthermore, studies described here propose a method for in situ recalibration of a biofouled sensor without necessitating removal of the sensor from the test environment. These studies have implications not only for oxygen sensors, but also for a wide variety of implantable electrochemical sensors.

First, polyeugenol (PE), which had been shown in previous work to be a promising polymer membrane for in vivo sensors, was electropolymerized onto individually addressable microelectrodes on a microelectrode array. The PE membrane was investigated for membrane coating uniformity and durability via potassium ferricyanide as a probe molecule. The PE membrane was proven to be permeable to oxygen through a calibration study, as well as uniformly covering the microelectrode surface through a probe molecule study. However, PE was shown to not be stable after 24 hours, as evidenced by the appearance of a ferricyanide electrochemical signal at this time point. Therefore, although permeable to oxygen, PE was not used for the duration of this work due to its instability over time.

Second, poly-o-phenylenediamine (PoPD) was investigated for use as a protective membrane. PoPD was shown to be permeable to oxygen, uniformly coated on the 2 mm gold macroelectrode, and stable over time. The PoPD membrane exhibited stability over time as shown through the probe molecule study with potassium ferricyanide. In addition, the PoPD-

coated electrode showed oxygen permeability and sensitivity over time in control electrolyte solution. This study also used a PoPD-coated and bare gold macroelectrodes to study the effects of biofouling when incubated in various foulant solutions over a period of 13-19 days. PoPD-coated electrodes exhibited more consistent sensitivity values when incubated in biofouling solutions than did bare electrodes. In addition, a study simulating an in vivo experiment calls into question current methods of calibrating in vivo sensors, as these data show significant changes of oxygen sensitivity when incubated in foulant solutions. This is the first study to my knowledge that quantifies the changes in sensitivity of an oxygen sensor due to biofouling. However, this work may not be directly applicable to in vivo sensors, as the reaction kinetics and fouling would be different between ex vivo and in vivo test environments. This study was a crucial experiment to prove the viability of PoPD as a protective polymer membrane coating for an in vivo oxygen sensor, as well as the first to quantify sensitivity changes due to biofouling of an oxygen sensor.

Third, PoPD was electropolymerized onto an individually addressable gold microband electrode on a microelectrode array. Microelectrodes are on a more feasible scale to apply as an in vivo sensor, as they would induce less tissue damage upon implantation than would the sensor using a macroelectrode in the previous study. The effects of biofouling were studied on a PoPD-coated microelectrode. In addition, a new method of in situ recalibration of a biofouled PoPD-coated microelectrode was proposed and its efficacy studied. The PoPD-coated electrode exhibited no appreciable change in oxygen sensivitiy when incubated in bovine serum albumin (BSA) solution; however, when incubated in fibrinogen solution, the PoPD-coated electrode exhibited a 16-33% change in oxygen sensitivity. The in situ recalibration method was able to effectively predict a new oxygen sensitivity for the fibrinogen-fouled PoPD-coated electrode to within 7% error of the experimental oxygen sensitivity value. This study serves as a proof-of-

concept for the in situ recalibration method; nevertheless, this is a profound result, and could have significant implications for a variety of implantable electrochemical sensors.

5.2 Future Work

The work described in this dissertation serves as fundamental research and application of polymer-coated gold electrode used for oxygen sensing. The future of this project requires fabrication of an in vivo probe. The probe, which was first designed by the Paul/Fritsch groups and Dr. Mengjia Hu, will be made out of SU8, an epoxy-based material that can be produced on the microscale via standard photolithography methods and provide tensile strength for clinical applications.[1-4] The design of the probe, shown in Fig. 5.1, has an implantable tip with dimensions of 7 mm long, 100 μm wide, 100 μm thick; the electrode array on the probe tip contains 9 active band electrodes of length 100 μm and width 4 μm, with 4 μm gap between electrodes. The microbands connect to an edge connector at the other end of the probe, making electrical connections to electrode leads of a potentiostat. This probe could be implanted in rat brain, and real-time oxygen levels can be monitored. Through use of this probe, the in situ recalibration technique described in this dissertation could recalibrate a biofouled in vivo oxygen sensor. In this way, the implanted probe would not need to be explanted and recalibrated in an external environment, improving the field of in vivo sensor calibration and function. In addition to oxygen, the in situ recalibration method described in this work could be applicable to a variety of other in vivo electrochemical sensors.

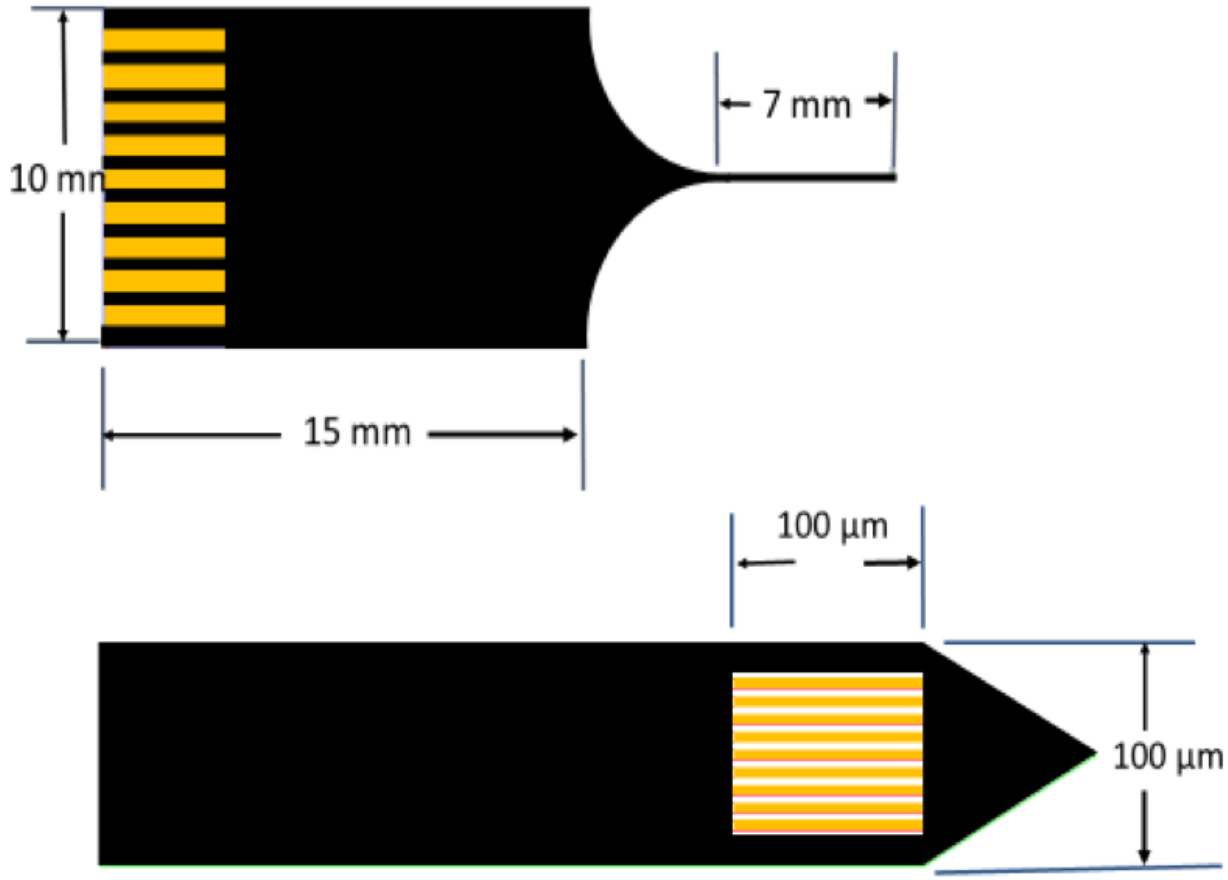

Figure 5.1 Probe design of microelectrode array; original design of Dr. Mengjia Hu and Dr. Ingrid Fritsch.

5.3 References

1. Altuna, A.; Gabriel, G.; Menendez de la Prida, L.; Tijero, M.; Guimera, A.; Berganzo, J.; Salido, R.; Villa, R.; Fernandez, L. J., SU-8-based microneedles for in vitro neural applications. *Journal of Micromechanics and Microengineering* **2010,** *20* (6), 064014/1-064014/6.

2. Xiang, Z.; Wang, H.; Pant, A.; Pastorin, G.; Lee, C., Development of vertical SU-8 microneedles for transdermal drug delivery by double drawing lithography technology. *Biomicrofluidics* **2013,** *7* (6), 066501/1-066501/10.

3. Tijero, M.; Gabriel, G.; Caro, J.; Altuna, A.; Hernandez, R.; Villa, R.; Berganzo, J.; Blanco, F. J.; Salido, R.; Fernandez, L. J., SU-8 microprobe with microelectrodes for monitoring electrical impedance in living tissues. *Biosens. Bioelectron.* **2009,** *24* (8), 2410-2416.

4. Ismailova, E.; Doublet, T.; Khodagholy, D.; Quilichini, P.; Ghestem, A.; Yang, S. Y.; Bernard, C.; Malliaras, G. G., Plastic neuronal probes for implantation in cortical and subcortical areas of the rat brain. *International Journal of Nanotechnology* **2012,** *9* (3-7), 517-528.